Thermodynamics and kinetics of conversion reaction in zinc batteries

Xianhong Chen, Xuefang Xie*, Pengchao Ruan, Shuquan Liang, Wai-Yeung Wong*, and Guozhao Fang*

Abstract

Aqueous zinc-based batteries (AZBs) based on the conversion-type mechanism have become a hot spot now due to their low cost, high safety and large capacity, which provides a significant opportunity for large-scale energy storage. However, conversion reactions in AZBs face serious thermodynamic and kinetic challenges. Rather than the common advances, this review focuses on fundamental aspects of reaction thermodynamics and kinetics for AZBs that lacks systematic attention and understanding. The conversion reaction mechanisms of AZBs including anode conversion reaction, manganese-based, chalcogenide-based, halogen-based, copper-based, and iron-based conversion reaction were discussed. The fundamental issues and perspectives of the battery system were further highlighted. The final section proposes significant directions to discuss how to better understand and design the effective conversion battery system via combining thermodynamics and kinetics.

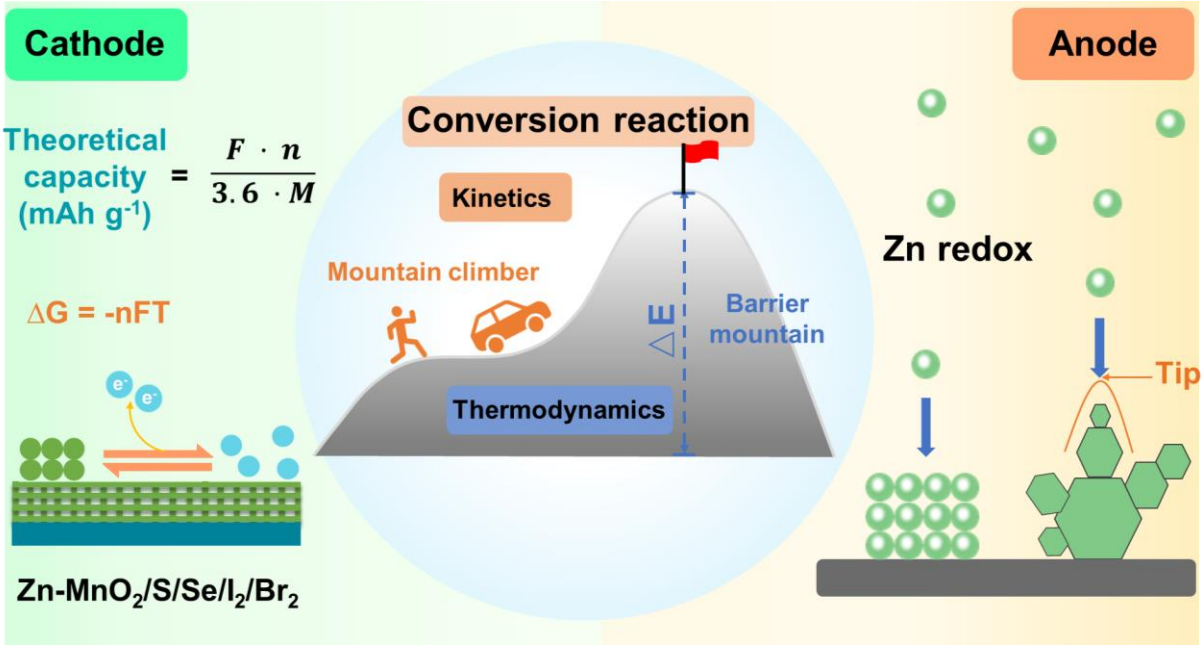

Aligned with the global trend towards green energy development, urgent action is required to accelerate the transformation and upgrade of energy storage systems with desirable characteristics such as high energy/power density, long-cycle stability, high energy conversion efficiency and affordability.[1, 2] Aqueous zinc-based batteries (AZBs) exhibit remarkable properties including high safety, high gravimetric capacity (820 mAh g^{-1}), and abundant zinc reserves, making them the subject of widespread concern.[3-5] AZBs based on the conversion-type mechanism of electrode materials, such as solid/liquid conversion, possess relatively high operating voltage and high theoretical capacity, representing a significant opportunity for stationary energy storage.[6, 7] There are many types of AZBs depending on this mechanism (**Table 1**), such as zinc-manganese (Zn-MnO_2) batteries,[8, 9] zinc-sulfur (Zn-S) batteries,[10, 11] zinc-selenium (Zn-Se) batteries,[12, 13] zinc-iodine (Zn-I_2) batteries,[14, 15] zinc-bromine (Zn-Br_2) batteries,[16, 17] zinc-copper (Zn-Cu) batteries,[18] zinc-iron (Zn-Fe) batteries.[19]

Despite the remarkable advances made in recent years, conversion-type AZBs remain far from maturity. In comparison to insertion-type reactions, the conversion-type reactions are less dependent on the framework of the electrode materials, but face significant challenges related to thermodynamics and kinetics (**Figure 1**),[7, 20, 21] primarily characterized by: (1) Thermodynamic instability of electrodes, electrolyte and interfaces. When more electron transfer of electrode is activated, it can provide higher specific capacity and larger electrode potential difference **(Figure 1a)**, which greatly increases the energy density of battery. However, high specific capacity is limited by conversion thermodynamics of electrode and stability of intermediate products. The decompositions of electrolyte such as hydrogen evolution reaction (HER) and oxygen evolution reaction (OER) are induced under these large energy output, because of the narrow electrochemically stable voltage window of aqueous electrolyte **(Figure 1b)**.[8] In addition, the issues including zinc dendrites,

corrosion, and passivation, can cause poor reversibility and stability of Zn anode **(Figure 1c)**. (2) Unsatisfactory kinetics of conversion reaction. The energy barrier of conversion reactions is usually high (**Figure 1d**), as it involves the phase difference between reactants and products. The reaction rate is greatly affected by the undesired redox activity of reactant and the accumulation of inactive products in electrode interfaces, thus result in severe polarization (**Figure 1e**). (3) Shuttle effect of intermediate products. The soluble ions generated at the cathode can shuttle to the anode side (**Figure 1f**), particularly for the chalcogen[22] and halogen reactants[23], resulting in self-discharge and capacity decay. These above issues could significantly affect the efficiency and service life of batteries.

Beyond that, some critical difficulties still plague this field such as the difficulty in revealing conversion-type reactions due to the complexity of reactants and products, the diversity of reaction paths. The electrochemical reaction process involves electron transfer, polarization, solvent effects, and interfacial side reactions, leading to a dearth of comprehensive knowledge regarding the underlying mechanisms of system reactions. Although some reviews offer advances and strategies for the conversion-type cathodes in AZBs,[7, 24, 25] the contents related thermodynamics and kinetics of conversion-type reactions are rarely reported. Based on the above discussion, a systematic and comprehensive understanding in this aspect is urgently. In this review, we summarized and discussed the conversion reactions in AZBs, primarily from the aspects of thermodynamics and kinetics. Based on this understanding, the fundamental principle and perspectives of the battery system were highlighted, followed by the guidance of future research proposals.

Table 1 Summary table of theoretical voltage, capacity and electron transfer number of conversion-type batteries.

Conversion type	Redox pairs	Theoretical voltage	Theoretical capacity (mAh g^{-1})	Electron transfer number

	(V, vs. Zn^{2+}/Zn)			
Solid phase	MnO_2/Mn^{2+} [9]	1.99	616	2
	I_2/I^- [23]	1.29	211	2
	I_2/I^+ [26]	1.83	211	2
	S/ZnS [27]	0.56	1675	2
	S/Cu_2S [28]	1.26	3350	4
	$Se/ZnSe$ [13]	0.63	678	2
	Cu^{2+}/Cu [29]	1.1	844	2
Liquid phase	Br_2/Br^- [17]	1.83	335	2
	Fe^{2+}/Fe^{3+} [30]	1.76	480	1

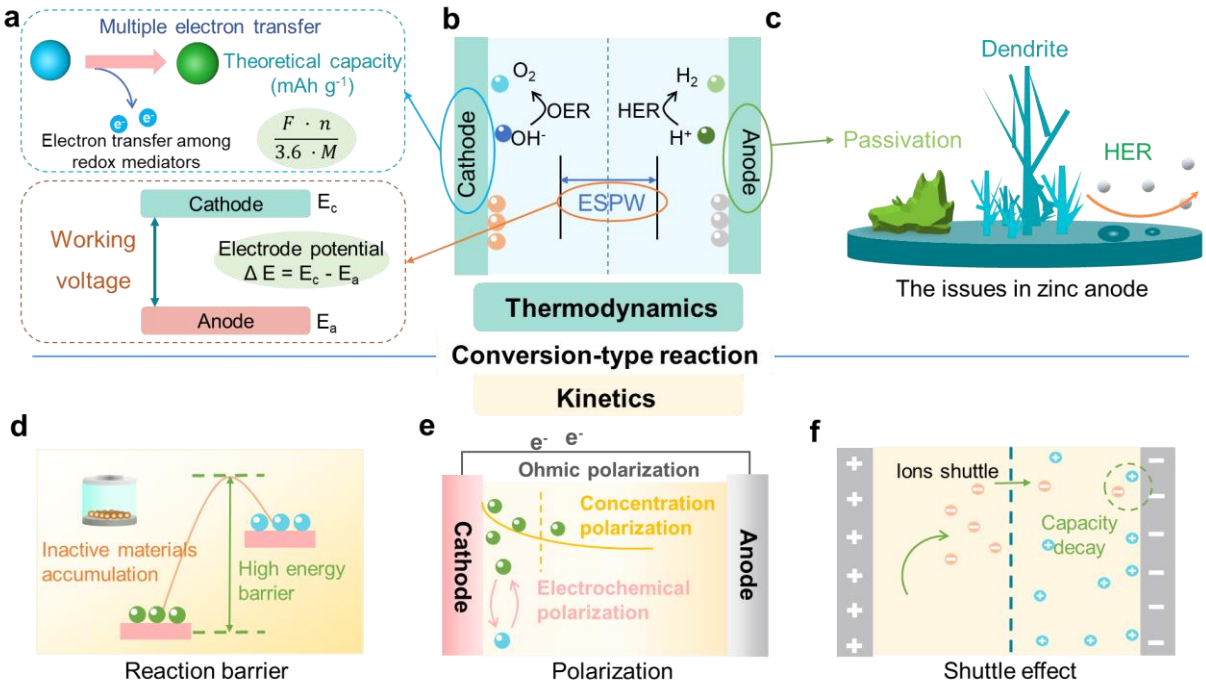

Figure 1. Illustration of thermodynamic and kinetics challenges for conversion-type reactions. (a) Calculation of thermodynamic capacity and voltage. (b) OER and HER of aqueous electrolyte. (c) Side reactions at the

anode side interface. The kinetics challenges of (d) high reaction barrier, (e) polarization and (f) shuttle effect.

Conversion reaction of anode materials.

The conversion-type anode materials include zinc metal anode and conversion-type zinc compounds. The zinc metal anode and its modified counterparts mainly leverage the plating/stripping of Zn^{2+}/Zn (solid-liquid conversion reaction) for energy storage.[31, 32] The reaction mechanism of conversion-type zinc compounds such as $2ZnCO_3 \cdot 3Zn(OH)_2$, is based on the conversion between zinc compounds and zinc metal, which is a typical solid-solid conversion reaction.[33] In this section, the reaction mechanisms of these conversion-type anodes will be discussed in detail. In particular, the issues caused by the characteristics of these reactions, the influencing factors and their modification strategies will also be analyzed in depth.

Solid-to-liquid reaction of zinc metal anode. The process of solid-to-liquid reaction in the zinc anode plating/stripping involves two electron transfers.[34] The reduction process of zinc ions in the electrolyte is the plating of Zn^{2+} on the anode, while during oxidation, the stripping process entails the oxidation of metal zinc to Zn^{2+}, expressed as follows[35]:

$$Zn^{2+} + 2e^- \leftrightarrow Zn\ (s) \qquad (1)$$

In alkaline electrolytes, Zn is oxidized to $Zn(OH)_4^{2-}$ during discharge, and then easily decomposed into inert ZnO, causing electrode passivation and hindering the uniform diffusion and deposition of Zn^{2+}.[36, 37] The reaction equations are as follows:

$$Zn^{2+} + 4OH^- \rightarrow Zn(OH)_4^{2-} \qquad (2)$$

$$Zn(OH)_4^{2-} \rightarrow ZnO + H_2O + 2OH^- \qquad (3)$$

Total equation:

$$Zn + 2OH^- \rightarrow ZnO + H_2O + 2e^- \qquad (4)$$

Dendrite formation occurs even at low capacities and moderate current densities in an alkaline environment, suggesting a thermodynamic instability. Also, the zinc anode is severely corroded in an alkaline environment, resulting in battery failure. Corrosion, passivation and shape change among Zn, $Zn(OH)_4^{2-}$ and ZnO, along with reactivity difference and structure framework correspond to the dynamic disadvantage and irreversibility of Zn anode.[31] To mitigate the issue, an effective method was proposed by Li et al.,[38] which converted ZnO powder into a nanoporous zinc electrode with a bicontinuous structure through a method like percolation dissolution. The ion conduction network of the Zn core/ZnO shell structure has strong stability, which can realize stable phase transition and maintain the reversible cycle of anode. In addition, the complexes can coordinate with Zn and avoid the generation of intermediate by-product like $Zn(OH)_4$.[39] In detail, the addition of complexing agent KBr changes the common solid-liquid-solid electrochemical conversion mode (Zn-$Zn(OH)_4^{2-}$-ZnO) to solid-liquid (Zn to Zn-Br), which achieves highly reversible conversion kinetics along with low polarization voltage because of reduced conversion barrier. This also can avoid the electrode passivation caused by ZnO precipitation that contributes to long cycle life.

In weakly acidic/neutral electrolytes, which is the main part of the discussion, the formation of zinc dendrites is associated with the diffusion behavior of Zn^{2+}, with the morphology of dendrite due to “tip effect” (**Figure 2a**).[33, 34] The presence of intrinsic inhomogeneity on the anode surface gives rise to Zn dendrite, particularly under high-capacity deposition. Abnormal growth of zinc dendrites is responsible for puncturing the membrane and shorting battery life. In response to this issue, a series of effective strategies such as 3D composite anode,[40, 41] surface-modify anode,[42, 43] eutectic alloy anode,[44, 45] etc. have been proposed. For instance, a longitudinal zinc-aluminum alloy anode with alternating Zn and Al sheet structures was proposed by Wang et al.,[46] in which the 2D Al nano-frame

can accommodate the deposition of zinc ion, and the insulating Al_2O_3 surface creates a charge-shielding effect that can limit the electroreduction of Zn^{2+} on the Al/Al_2O_3 patterns, thus promoting the uniform electrodeposition of Zn^{2+} on the precursor Zn sites. Interestingly, Mu et al.[40] proposed a 3D multichannel carbon array (3D-FGC) anchored by nitrogen-doped graphene nanofibers (GFs), which exhibits a significantly larger specific surface area and porosity, facilitating the minimization of local current density on the surface and thereby achieving uniform electric field distribution to modulate Zn^{2+} deposition. Ultimately, a Coulombic efficiency of 99.67% is maintained even after 3000 cycles at a current density of 120 $mAcm^{-2}$. The 3D composite electrode, equipped with rapid ion transport channels, represents an effective strategy for enhancing the diffusion rate of Zn^{2+} and controlling their nucleation and growth kinetics, thereby enabling the fast reaction kinetics. Other typical examples for addressing the dendrite formation have been well summarized and discussed in some review articles.[47, 48]

In addition to dendrite growth, the hydrogen evolution reaction is also of great concern:

$$2H^+ + 2e^- \rightarrow H_2 \quad (5)$$

$$2H_2O + 2e^- \rightarrow H_2 + 2OH^- \quad (6)$$

Active H_2O is one of the main factors that trigger the hydrogen evolution reaction at the electrode interface. Due to the lower electrode potential of Zn^{2+}/Zn (-0.76 V *vs.* SHE) compared to H^+/H_2 (0 V *vs.* SHE), H_2O is more prone to undergo electrolysis during the charging process, rather than the reduction of Zn^{2+} to Zn (**Figure 2b**).[31, 49] This sequence of events exacerbates the change in OH^- concentration, which can react with SO_4^{2-} and Zn^{2+} to form insoluble and insulating by-product $Zn_4(OH)_6SO_4 \cdot nH_2O$ (ZSH) due to the solubility product constant (K_{sp}) of ZSH is much less than that of $Zn(OH)_2$.[49] It ultimately reduces the Coulombic efficiency and battery life. Mitigating the reactivity

of free water and optimizing the solvation structure of Zn^{2+} are the common strategies for improving electrochemical stability of Zn anode[50-52]. For example, zinc-friendly Lewis base solvent containing a lone pair of electrons, such as N, N-dimethylformamide (DMF), can make Zn^{2+} preferentially coordinate with and replace the part of the Zn^{2+} solvation sheath H_2O molecule, leading to the Zn^{2+} solvation structure optimization.[53] The lone pair of electrons with unique electron-attracting characteristics can interact with H_2O to form intermolecular hydrogen bonds, which can destroy the original hydrogen bond network, inhibiting the reactivity of free water. Similarly, introducing anions like with iodide and chloride ions with electron-donating ability to form water-less $ZnI(H_2O)^{5+}$ [54] or anhydrous $ZnCl_4^{2-}$ [55] structures achieves the same effect by weakening the charge transfer between Zn^{2+}-H_2O. Changing the solvation effect of Zn^{2+} also reduces the de-solvation energy of Zn^{2+}, which is conducive the rapid ion transfer in the interface, thereby increasing the reaction rate.[56]

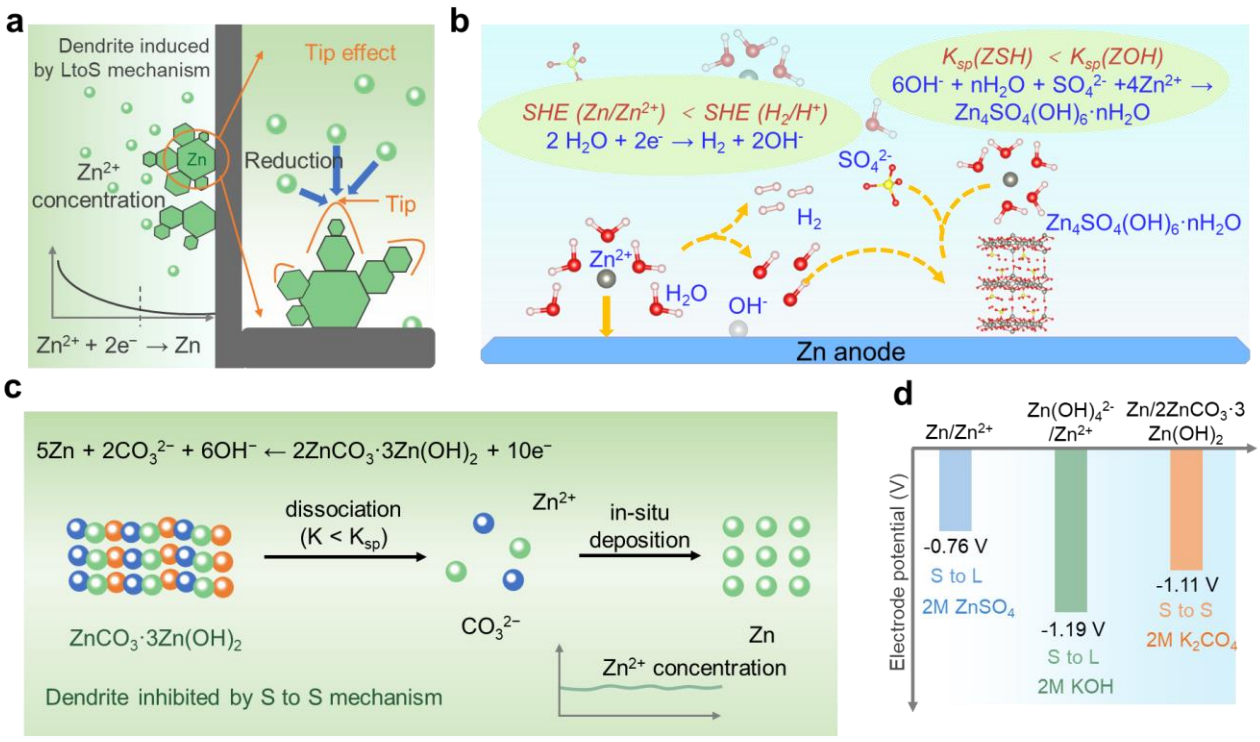

Figure 2. The reaction state of zinc anode in different electrolytes. (a) Schematic diagram of dendrite growth caused by DLA in the Zn/Zn^{2+} reaction. (b) The de-solvation process and corresponding side reactions

occurring at the zinc anode interface. Reused with permission from ref 49. Copyright 2021 Elsevier. (c) StoS reaction process of $2ZnCO_3 \cdot 3Zn(OH)_2$. (d) Summary of electrode potentials of zinc anode StoS and StoL reactions.

Solid-to-solid reaction of zinc compound anode. The dendrite formation induced by diffusion-limited aggregation (DLA) is a challenge to be addressed in the electrochemical reaction at the Zn interface based on the typical solid-liquid transformation mechanism.[31] For this point of view, a solid-solid conversion between a slightly soluble salt and a metal is proposed,[33] which is mainly borrowed from lead-acid batteries.[57] It mainly realizes the charge-discharge process through the transport of anions rather than the diffusion of anions, avoiding the zinc dendrite generation. This solid-solid conversion mechanism fundamentally inhibits the growth of dendrites triggered by DLA effect from solid-liquid reactions.

Alkaline carbonate $2ZnCO_3 \cdot 3Zn(OH)_2$ retains structural stability in neutral and weakly alkaline environments, showing a potential reaction medium for solid-solid reactions without DLA effect. Chao et al.[33] proposed the detailed electrochemical process of $2ZnCO_3 \cdot 3Zn(OH)_2$ and found that free Zn^{2+} is deposited around $2ZnCO_3 \cdot 3Zn(OH)_2$ during the charging process, with additional dissociation of basic zinc carbonate supplementing the consumed Zn^{2+} to maintain balance. During discharging, dissociated Zn^{2+} reacts with CO_3^{2-} and OH^- to produce $2ZnCO_3 \cdot 3Zn(OH)_2$ crystals correspondingly (**Figure 2c**):

$$2ZnCO_3 \cdot 3Zn(OH)_2 + 10e^- \leftrightarrow 5Zn + 2CO_3^{2-} + 6OH^- \quad (7)$$

Zinc anchored in situ during this StoS process eliminates the DLA effect. However, it should be noted that the electrochemical redox process of Zn^{2+} is limited by the dissociation rate of

$2ZnCO_3 \cdot 3Zn(OH)_2$. Meanwhile, the high energy barrier of solid phase reaction and the electrochemical polarity caused by the StoS reaction at the interface would affect the reaction kinetics, requiring for further optimization.[1, 7]

Discussion of solid-to-liquid and solid-to-solid reactions. Solid-liquid conversion demonstrates inherent differences compared to solid-solid conversion. From a thermodynamic perspective, the standard electrode potential of zinc anode conversion is -0.76 V *vs.* SHE (Zn/Zn^{2+}), -1.19 V *vs.* SHE ($Zn^{2+}/Zn(OH)_4^{2+}$) and -1.11 V *vs.* SHE ($Zn/ZnCO_3 \cdot 3Zn(OH)_2$) **(Figure 2d)**.[33, 58] According to the relationship between Gibbs free energy (ΔG) and electrode potential:

$$\Delta G = -nFE \qquad (8)$$

ΔG represents the standard Gibbs free energy change, n is the number of moles of transferred electrons, F is the Faraday constant (96485 C mol^{-1}), and E is the standard electrode potential. It indicates that the StoS and StoL of Zn metal is feasible, with a strong tendency to oxidize and release electrons. However, they are different in terms of thermodynamic evolution. The StoL reaction, primarily limited by diffusion polarization, is influenced by the transport kinetics and de-solvation of Zn^{2+}, as well as the platting/stripping rate at the electrode interface. The StoS reaction, mainly restricted by electrochemical polarization, relies on the dissociation/formation of basic zinc carbonate, which avoids the DLA effect while increasing the energy barrier for reversible reaction.

For the dynamic perspective, the StoL reaction necessitates considerations of ion diffusion and transmission, solvation effects, and plating/striping efficiency.[21] In detail, the selective aggregation of ions diffusion is the driving force behind the formation of zinc dendrite. Prior to Zn^{2+} electrodeposition, de-solvent is required thus the low de-solvation energy is beneficial for achieving rapid and reversible electrochemical reaction. Overall, the migration kinetics of Zn^{2+} can be described

as following equation:

$$K = \sum_I \frac{(Z_i)^2 F C_i}{6\pi\eta r_i} \qquad (9)$$

Where Z_i and C_i are the charge number and molar concentration of *i* ion, respectively. F is the Faraday constant, η is the viscosity of the electrolyte and r_i is the solvation radius of *i* ion. Therefore, in order to enhance the kinetics of zinc conversion, optimizing the solvation structure and zinc ion diffusion rate are considered beneficial. In contrast, StoS reactions rely on the reversible dissociation/formation of redox pairs (e.g., basic carbonates), where electrochemical polarization plays a critical role in facilitating fast and reversible electrochemical reactions. This necessitates redox pairs with low reaction energy barrier. Additionally, there may be a competition for electrons involving Zn/Zn^{2+} reaction due to the existing of Zn^{2+}.

Conversion-type zinc batteries based on cathode materials.

The process of conversion mechanism occurs via a redox reaction involving a change in valence state, rather than relying on the Zn^{2+} intercalation in host tunnel.[59] The versatility of conversion reaction can be mainly categorized into three major types: liquid-liquid, solid-liquid and solid-solid conversion. The redox reactions in liquid-liquid reactions rely on conversion among redox active ions, where concentration polarization has a significant impact, and necessitating the consideration of ion shuttle issue. Solid-liquid and solid-solid reactions require overcoming high energy barriers for phase transitions, and swelling of electrodes or broken particles that can cause battery capacity decay. Various battery systems based on conversion reactions are discussed as follow.

Zinc-manganese batteries. Zn//manganese batteries have attracted a lot of attention due to their low cost and high safety.[60] Zn//MnO_2 battery with mild electrolyte originally invented by Takayuki

Shoji in Japan in the 1880s.[61] By 2011, Xu and Kang et al.[62] proposed the concept of secondary zinc-ion batteries, in which Zn^{2+} are inserted into MnO_2 cathode and undergo a classic Zn^{2+}-(de)intercalation mechanism (**Equation 10**). During charging, Zn^{2+} dissociate from the cathode and subsequently re-insert in the next charge. Later, some reports indicated that the charge storage process is mainly dominated by the H^+ insertion to form H_xMnO_2 rather than Zn^{2+} insertion (**Equation 11**), because of smaller size and superior kinetics.[63, 64] Meanwhile, H^+/Zn^{2+} co-intercalation mechanism was also proposed.[65, 66]

Zn^{2+} de-intercalation mechanism $\quad Zn^{2+} + 2e^- + 2MnO_2 = ZnMn_2O_4$ (ZMO) $\quad$ (10)

H^+ de-intercalation mechanism $\quad xH^+ + MnO_2 + xe^- = H_xMnO_2$ $\quad$ (11)

In 2016, Pan and Liu et al.[63] first reported a Zn//MnO_2 battery based on a conversion reaction between MnO_2 and MnOOH/$ZnSO_4[Zn(OH_2)]_3 \cdot xH_2O$. The limited electron transfer (e.g., $1e^-$ for Mn^{3+}/Mn^{4+}) is not conducive to the development of high energy density zinc batteries. By 2019, Chao et al.[9] proposed the conversion chemistry of Mn^{2+}/MnO_2 in a strong acidic electrolyte involving a $2e^-$ transfer reaction (**Equation 12**). Compared to that in near-neutral aqueous electrolyte, this conversion chemistry provides high theoretical voltage of 1.99 V *vs.* Zn^{2+}/Zn, and a high theoretical capacity of 616 mAh g^{-1} (**Figure 3a**). When combined with an alkaline anode, high voltage output can be achieved. Yadav et al.[67] designed Mn^{2+}/MnO_2 and Mn^{2+}/MnO_4^- conversion and successfully achieved an output voltage of 2.45 V and 2.8 V *vs.* $Zn^{2+}/Zn(OH)_4^{2+}$, respectively. According to the Nernst equation (**Equation 13**), the increase in proton concentration results in an elevation of the positive electrode potential, facilitating the attainment of higher output voltage (**Figure 3b**). This dissolution-deposition reaction mechanism is not controlled by the stability of the material framework, along with higher effective ion transfer number.

$$Mn^{2+} + 2\ H_2O \rightarrow MnO_2 + 4\ H^+ + 2e^- \quad (12)$$

$$E = E^{\theta} + \frac{RT}{nF} ln \frac{c^4(H^+)}{c(Mn^{2+})} \quad (13)$$

The previous perspectives on energy storage in MnO_2 systems maintain that intercalation reaction predominantly occurs in weak acid electrolytes, while dissolution-deposition reactions primarily take place under strong acid conditions.[59, 68, 69] However, Wu et al.[70] employed Mn K-edge XAS technology to investigate the redox behavior of Zn-Mn batteries in weak acid aqueous electrolyte, and revealed that approximately 50% of Mn from the cathode is dissolved to form Mn^{2+} at the conclusion of the initial discharge. Moreover, the majority of dissolved Mn is redeposited in solid form during charging, underscoring the inescapable contribution of MnO_2 dissolution and deposition to the overall capacity even under weak acid conditions (**Figure 3c**).[71, 72] Furthermore, some researchers proposed a reversible $Zn_4SO_4(OH)_6$ (ZSH)-assisted dissolution/deposition reaction (**Equation 14**).[73] The conversion efficiency between $Zn_xMnO(OH)_2$ nanosheets and ZSH serves as the critical factor in determining the reversibility and stability of Zn-Mn batteries (**Figure 3d**).

ZSH-assist reaction: $Zn_4SO_4(OH)_6 \cdot 4H_2O + Mn^{2+} \rightarrow Zn_xMnO(OH)_2 + 4H^+ + SO_4^{2-} + 2e^-$ (14)

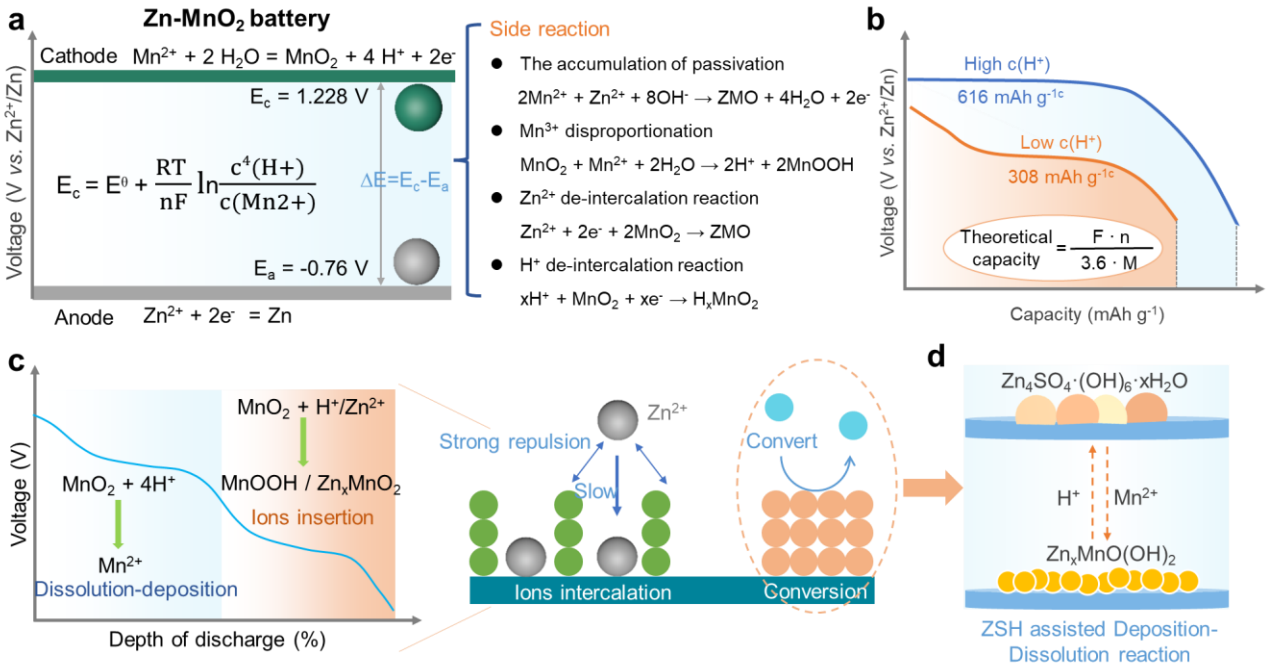

Figure 3. Reaction mechanisms of Zn-MnO_2 battery. (a) Typical reaction mechanism and side reactions of Zn-MnO_2 battery. (b) Predicted capacity of Zn-MnO_2 battery under different c(H^+). (c) The contribution interval of ion intercalation and dissolution-deposition to capacity under weak acid conditions. (d) ZSH-assisted conversion reaction mechanism.

Nowadays, it is generally believed that the Mn^{2+}/MnO_2 dissolution/deposition reaction contributes a significant amount of capacity even in weakly acidic electrolytes. However, an undeniable fact is that this energy storage mechanism of Zn-MnO_2 battery is greatly affected by the diversity of manganese structures (including α-, β-, γ-, δ-, ε-, λ- and amorphous phase), electrolyte composition and special adjuvants, which still needs to be further explored. Nevertheless, it is feasible to optimize the kinetics and thermodynamic characteristics of the electrochemical reaction by implementing effective strategies, for the sake of enhancing the energy efficiency and output of battery.

Regulating ion behaviors for excellent conversion kinetics. It should be noted that the

Mn^{2+}/MnO_2 dissolution/deposition mechanism heavily relies on the dissolution deposition of Mn^{2+} on the current collector. However, after undergoing multiple cycles, the built-up of passivation products such as Zn_xMnO_2 will lead to electrode passivation and a gradual decline in capacity.[74] To counteract this undesirable consequence, the reactivation of the electrode can be achieved through either external acid-assisted dissolution[74] or the introduction of a redox mediator such as iodine[75], aiming at facilitate the kinetics and "restoring" the capacity. In comparison to Mn, iodine exhibits a lower potential and smaller overpotential in comparison to Mn, signifying its good capability to reduce MnO_2 and its superior kinetics. More specifically, the discharge-derived I^- facilitate the reduction of solid MnO_2, generating Mn^{2+} and subsequently undergoing oxidation to form I_3^- (**Equation 15, 16 and 17**). These I_3^- ions are then discharged and reduced back to I^- ions on the electrode surface, thus completing a full mediator cycle (**Figure 4a**). This mediator-based strategy demonstrates enhanced discharge capacity and cycling stability, as evidenced by its performance of over 225 cycles at a current density of 15 mAh cm^{-2}. Bromine redox mediator and acetate has also been found to have a similar mechanism.[76, 77] The media ions improve the conversion rate and reaction reversibility of manganese dioxide through synergistic effects, improving battery capacity and cycle stability.

$$\text{Ionization of } I_2\text{: } I_2 + 2e^- \rightarrow 2I^- \qquad (15)$$

$$\text{Restore } MnO_2\text{: } MnO_2 + 3I^- + 4H^+ \rightarrow Mn^{2+} + I_3^- + 2H_2O \qquad (16)$$

$$\text{Restore } I_3^-\text{: } I_3^- + 2e^- \rightarrow 3I^- \qquad (17)$$

The deposition products have been confirmed to be mainly influenced by Zn^{2+} during the manganese deposition process. The presence of Zn^{2+}, which possesses a solvation structure similar to that of Mn^{2+}, can induce the formation of inert compounds through Zn^{2+} and Mn^{2+} co-deposition.[63,

[78] To address this issue, Hu et al.[79] propose a novel quasi-eutectic electrolyte, in which the urea molecules replace OTf^- species at the MnO_2 interface (**Figure 4b**). In addition, by virtue of the disparity in polarizability resulting from the alteration in the number of electrons in the outer orbital, urea exhibits a greater affinity for entering the solvation structure of Zn^{2+}, rather than that of Mn^{2+}. This impedes the de-solvation process of Zn^{2+}, augmenting the interfacial de-solvation kinetics of Mn^{2+} and enabling the uniform and reversible deposition of manganese at the interface.

The manganese deposition is also susceptible to interference from the concentration of interface ions, particularly H^+, who determines the potential and capacity of battery.[80] According to this characteristic, highly efficient manganese deposition can be promoted by controlling the behavior of interfacial H^+. A series of electrolytes containing proton buffers such as CH_3COO^- [81], $H_2PO_4^-$[82] and BF_4^- [83]etc. have been proposed. These proton buffers maintain the interfacial H^+ concentration to regulate the efficiency of manganese dissolution/deposition reaction (**Figure 4c**). However, it also found that a balance of for maintenance of interfacial H^+ concentration and steric hindrance of Mn^{2+} migration is necessary for optimal thermodynamics and kinetics. In specific, the steric hindrance to Mn^{2+} migration mainly involves the hindrance caused by solvated anions and the energy barrier associated with Mn^{2+} de-solvation. Anions with greater electron donor groups tend to be adsorbed at the cathode interface and adjust the H^+ concentration by forming hydrogen bonds. However, the larger size of groups can reduce the adsorption density, leading to electrostatic repulsion of positively charged Mn^{2+} at the cathode interface and significant steric barriers to migration. The $HCOO^-$ demonstrates a favorable balance between the interfacial H^+ concentration and the steric hindrance to solvated Mn^{2+} migration. [20] This allows the interface to maintain stable output capacity and thermodynamic stability while effectively regulating the chemical coordination and solvation

behavior of Mn^{2+}, ultimately achieving excellent transformation kinetics (**Figure 4d**). Additionally, the de-solvation behavior of Mn^{2+} governs the kinetics of MnO_2 dissolution/deposition. High Mn^{2+} de-solvation energy contributes to high the steric migration barrier, leading to reduced transformation kinetics. Consequently, Liu et al.[20] proposed the incorporation of formic acid anions to balance the H^+ concentration at the interface and the migration resistance of sterically solvated Mn^{2+}, thus stimulating the rapid de-solvation process of Mn^{2+}. Moreover, reaction kinetics can also be promoted through doping strategies to increase the electronic conductivity of the cathode and lower the reaction energy barrier, such as fluorine doping and nickel doping.

Increasing effective dissolution-deposition chemistry. Enhancing the conversion efficiency of 2e-transfer dissolution/deposition chemistry is pivotal in advancing energy improvements. The introduction of weak acid ions, such as Ac-, into the weak acid electrolyte proves to be advantageous. By virtue of the lower Gibbs free energy of HAc compared to free H^+ (H_2SO_4), the inclusion of Ac^- facilitates the absorption of H^+ generated during the Mn^{2+} deposition process, thereby reducing the reaction potential of MnO_2/Mn^{2+}.[76] These alterations promote the deposition of Mn^{2+} and amplify the capacity contribution of dissolution/deposition chemistry (**Figure 4e**). Alternatively, the implementation of a hydrogel electrolyte with high cross-linking density (HCH) can delay the migration of H^+ to cathode, restraining the ion intercalation reaction that competes with the dissolution-deposition reaction.[71] Consequently, the MnO_2/Mn^{2+} system attains reversibility in the cyclic reaction, enabling a stable cycle of over 7,000 times.

Furthermore, it is well-established that acidic electrolytes facilitate the reversible transformation of MnO_2, while zinc anodes exhibit a lower potential in alkaline electrolytes. To enable the coexistence of both electrolytes and achieve concurrent optimization of redox chemistry for enhanced

energy output, decoupled battery systems have been proposed.[84] However, the utilization of electrolytes with distinct properties leads to ion cross-over effects, thereby demanding a sufficient supply of ions to maintain charge balance for efficient electron transfer. To address this issue, a three-compartment decoupled battery design was proposed.[85] The acidic catholyte and alkaline anolyte are isolated by a neutral potassium sulfate solution. During charging and discharging processes, potassium ions and sulfate ions traverse an ion-selective membrane to reach the anolyte and catholyte, respectively, ensuring proper charge balance and mitigating ion cross-over effects (**Figure 4f**). Consequently, this setup enables the attainment of high voltage (2.83 V) and impressive energy output (1,621.7Wh kg_{MnO2}^{-1}). Additionally, the integration of a flow device that facilitates electrolyte renewal within the decoupled system alleviates concentration polarization at the electrode-electrolyte interface, for better battery stability and rate capability.[86]

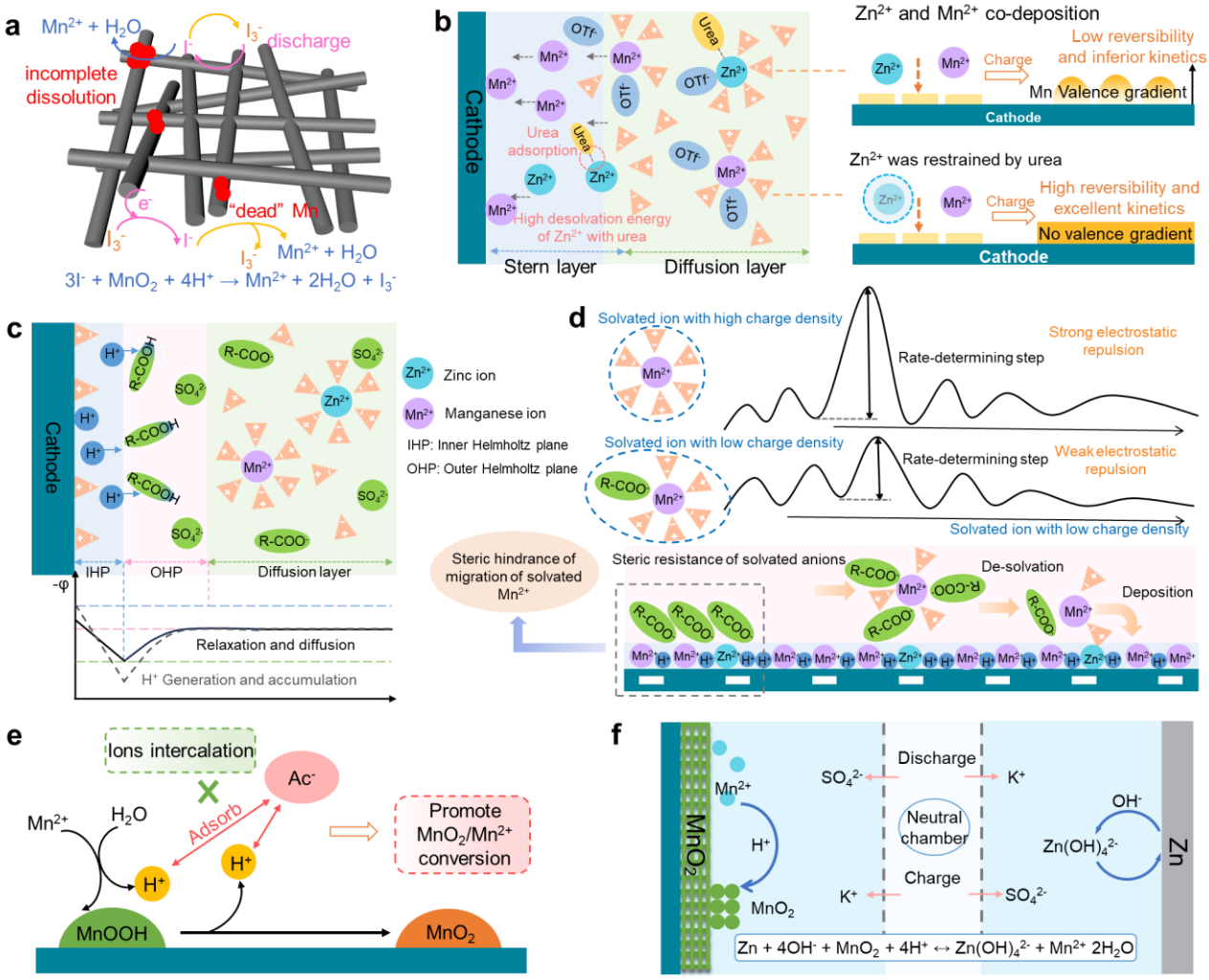

Figure 4. Challenges and optimization strategies for Zn-MnO_2 batteries. (a) Conceptual diagram of KI as a redox mediator that promotes the dissolution process of MnO_2. (b) Electrochemical behavior of urea-based eutectic electrolyte at cathode interface. (c) Electric double layer model of cathode-electrolyte interface controlled by $R\text{-}COO^-$ to thermodynamically increase capacity and (d) Adjust the interface electric field and ion solvation structure to improve reaction kinetic. (e) Schematic diagram of Ac-promoting manganese dissolution-deposition process. (f) Working mechanisms of three-chamber decoupled Zn-MnO_2 battery.

Zinc-sulfur batteries. Zn//S battery, with the advantages of natural abundance of sulfur, capitalizes on the solid-to-solid conversion reaction between S and ZnS for efficient energy storage (**Figure 5a**).[11, 27] This double-electron transfer reaction displays an conspicuous theoretical specific

capacity of 3350 mAh gs^{-1} and energy density of 572 Wh kg^{-1}.[28] However, the poor electronic conductivity of S (10^{-7} S cm^{-1}) and ZnS (10^{-9} S cm^{-1}), and their slow solid-to-solid conversion kinetics results in high overpotential and rapid capacity decay of the battery (**Figure 5b**).[8] In addition, the accumulation of uneven inactive products, the disproportionation, precipitation and dissociation of hydrogen sulfide, as well as the polysulfide shuttle also challenge zinc-sulfur batteries.[10, 28, 87] For addressing these issues, the strategies such as introducing redox media, optimizing battery configuration, and modifying cathode materials are summarized and discussed in this regard.

Introduce redox media for optimizing reaction behavior. Redox mediators (RMs) are a class of compounds that utilize their electrochemical redox properties to facilitate or regulate the behavior of electrochemical conversion reactions. For instance, the formation of intermediate species with charge carriers to enhance the efficiency of the conversion reaction, or the alteration of the conversion type of active ions (from StoS to StoLtoS) to achieve higher conversion kinetics.[6] Specifically, the former is to serve the mediators with higher redox potentials (e.g., 0.8 V for $Fe^{II}(CN)_6^{4-}/Fe^{III}(CN)_6^{3-}$) as a cationic bridge, which allows for the insertion of Zn^{2+} to form complex ions (**Figure 5c**), and enhances Zn^{2+} transfer rate and the reactivity towards S.[88] It effectively accelerated the conversion kinetics between sulfur and zinc sulfide, alleviating the voltage hysteresis issue. The latter one is to introduce of RMs with dual media functionality like quaternary ammonium iodide ($R_4N^+I^-$), with represented by trimethylphenyl ammonium iodide ($Me_3PhN^+I^-$).[89] The R_4N^+ cations can induce the formation of soluble polysulfides such as S_6^{2-} and S_4^{2-}, and then rapidly combine with Zn^{2+} to form ZnS. The R_4N^+ serves as dissolution mediator to generate soluble intermediates, for the sake of transforming the original S - ZnS (StoS) into S - $(R_4N^+)_2(SX)_2$ - ZnS (StoLtoS) conversion (**Figure 5d**), which largely facilitates the reaction kinetics. What's more, the iodide anion serves as the redox

mediator with I_3^-/I^- redox couple for the charge conversion process of ZnS-S, and the solubility of $R_4N^+I_3^-$ is low that helps in preventing the shuttling of polyiodide. These two strategies primarily optimize the reaction kinetics by reducing the reaction energy barrier, leading to a decrease in the reaction overpotential.

On the other hand, the theoretical capacity of S_2^-/S with two-electron conversion is limited, which hinders the development of high-energy-density batteries. In order to address this issue, a deep eutectic solvent (DES) electrolyte containing LiCl and H_2O (referred to as ZL-DES·5H_2O) is designed to activate CuS electrode and enable a four-electron transfer reaction (Cu^{2+}&S + Zn^{2+} + $4e^-$ ↔ Cu + ZnS) (**Figure 5e**), consisting of new oxidation-reduction pathways for copper (Cu → Cu_2S → $CuCl_2^-$ → $CuCl_4^{2-}$) and sulfur (ZnS → S_n^{2-} → S, n ≥ 4), which not only enhances the kinetics of conversion reaction but also effectively improves the output capacity and voltage of the battery.[90] It is worth noting that the stability of Cu^{2+} intermediate requires the high coordination effect of Cl^- to support. In addition, strategies involving continuous conversion (S↔CuS↔Cu_2S)[91], cascade conversion with solid-solid (S+2Cu^{2+}+2Zn→Cu_2S+2Zn^{2+}) and solid-liquid (Cu^{2+}+xO_2+Zn→(1-4x) Cu+2x Cu_2O+Zn^{2+})[92] also contribute to multi-electron transfer, for the sake of achieving high energy output.

Designing decoupled battery configuration. The decoupling of dual electrolytes in batteries allow for the optimal redox reactions of the cathode and anode, while effectively suppressing shuttle behavior of polysulfides (**Figure 5f**). The separation of electrolytes is typically achieved using ion exchange membranes[10, 93] and gel/solid electrolytes[28]. They achieve charge balance between the electrolytes through mediator ions exchange. For instance, Cai et al.[93] designed a zinc-sulfur decoupled battery with a S/Cu_2S cathode and Zn/$Zn(OH)_4^{2-}$ anode, where the $4e^-$ transfer reaction of

S/Cu_2S and the dual electrolyte system endowed the battery with high capacity and high voltage output. However, the volume of decoupled battery is large, and the high sulfur loading of active materials are crucial for achieving high energy density. The high sulfur loading contributes to high capacity, but the augmentation in volume or mass of electrode materials leads to a concomitant rise in the proportion of passivated material, thereby engendering an undesirable deceleration in kinetics. The potency of this detrimental effect is influenced by various factors including material activity, specific surface area, and electrolyte accessibility. In this regard, a magnetically induced high-sulfur-content cathode with a vertically aligned structure was developed.[10] The vertically assembled nanosheet network can facilitate rapid electron and ion conduction within thick sulfur electrodes, thereby enhancing the conversion kinetic. In conjunction with a Na^{2+}-coordinated polymer membrane with high ion selectivity that allows fast ions exchange, successfully achieving high energy output (53.2 mWh cm^{-2}).

Highly active cathode promoting conversion reaction. Electrode optimization can be divided into two parts of promoting conversion kinetics and improving energy density. The former is mainly achieved by enhancing ion transport speed and modifying electrode activity, such as loading carbon nanotubes to increase specific surface area,[27] using iron atoms for bidirectional catalysis to promote rapid S-ZnS conversion,[94] and designing Se/S composite materials to optimize conductivity and reactivity of cathode.[95] Among them, the design of Se/S cathode is a common approach because Se can adjust the electron density distribution and band structure of S, which in turn improves its conductivity and reactivity **(Figure 5g)** [11, 96]. This reduces the energy barrier between redox products, and achieving excellent cathode conversion kinetics. In addition to conventional material composite strategies, Zhi et al.[22] proposed an "ionic liquid (IL)" activation strategy for S cathodes **(Figure 5h)**.

They utilized lithium polysulfide as the cathode instead of solid sulfur, and introduced PEDOT:PSS as a support network, with IL serving as the active site. The $CF_3SO_3^-$ in IL acts as a transfer channel for Zn^{2+}, possessing high transfer rates and reactivity. This stable, porous and highly active cathode has resulted in exceptional conversion kinetics.

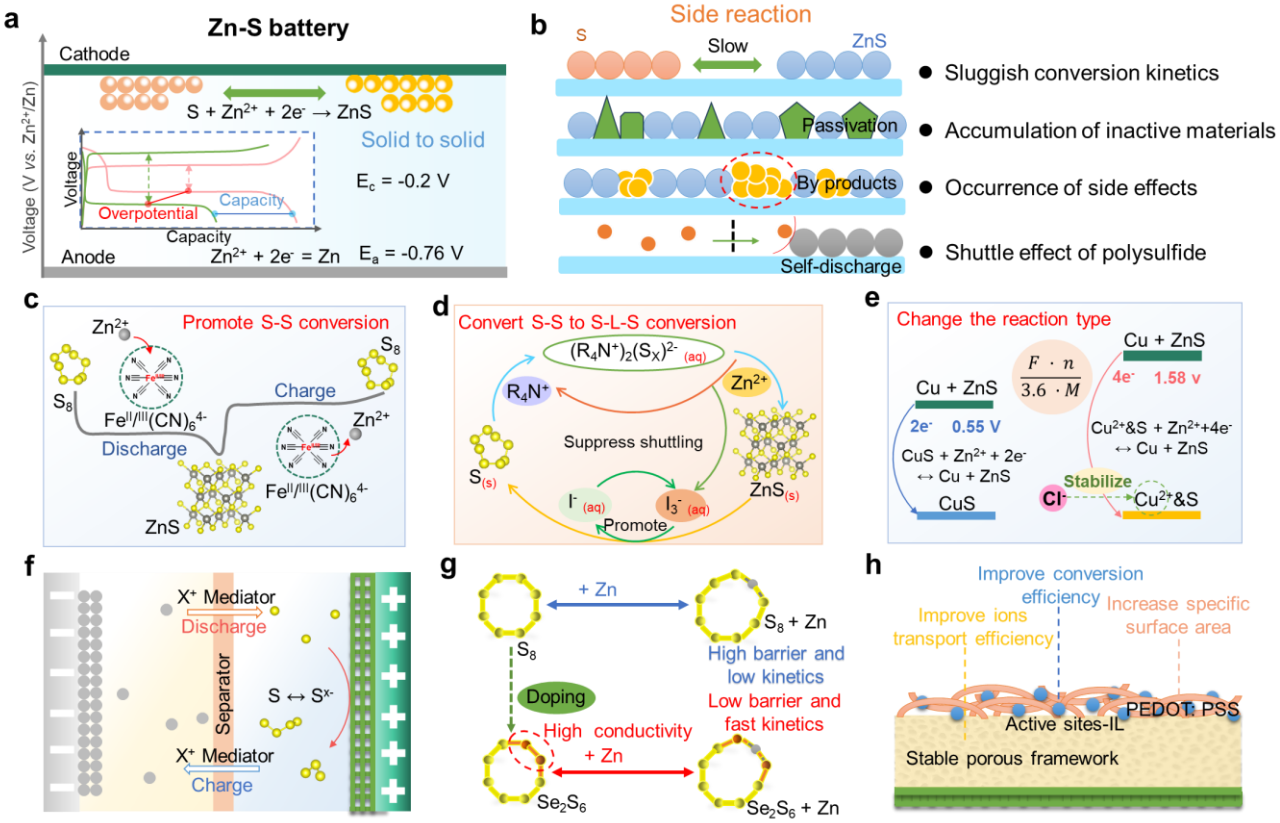

Figure 5. Reaction mechanism, side reactions and optimization strategies of zinc-sulfur batteries. (a) a conceptual illustration of typical zinc-sulfur battery and (b) the side reaction encountered. Optimize conversion reaction behavior by introducing redox mediators to (c) promote S-S conversion kinetics, (d) convert S-S to S-L-S conversion reaction and (e) change the S-S reaction type. (f) Decoupled battery for optimal redox reaction. (g) Se doping strategy increases the conductivity of S and lowers the reaction barrier. (h) Schematic illustration of liquid-film optimized LF-PLSD cathode.

Zinc-selenium batteries. With an electrical conductivity of 1×10^{-3} S m^{-1} and a theoretical

volumetric capacity of 3253 mAh cm^{-3}, selenium exhibits the potential for constructing zinc batteries with high volumetric energy density.[97] The typical reaction process of Zn-Se batteries involves the conversion of Se to ZnSe.[13]

$$Se + Zn^{2+} + 2e^{-} \leftrightarrow ZnSe \quad (18)$$

Se, being a member of the sulfur element family, exhibits resemblances in both its physical and chemical properties to S, as well as similar conversion reaction mechanism. Correspondingly, they face similar challenges such as the poor electronic conductivity, slow conversion kinetics, inactive products accumulation and side reaction. The energy barrier for solid-solid conversion between Se and ZnSe is high and the electron transport capability of the Se is weak, resulting in unfavorable reaction kinetics.[12, 97] Therefore, several studies have utilized composite material strategies, exemplified by the synthesis of porous nickel selenide loaded with carbon nanotubes,[98] Se-S solid solution and its composites,[95] amorphous Se doped with transition metal Ru.[99] These approaches for augmenting the conversion rate fundamentally through three aspects: bolstering the number of active sites, enhancing conductivity and increasing reactivity. Additionally, in order to essentially break through the theoretical capacity bottleneck, introducing auxiliary ions such as redox-active Cu^{2+} to facilitate multiple electron transfer reaction represents a viable strategy for breaking through theoretical capacity limitations.[12] In this context, Cu^{2+} enables four-electron transfer via the sequence reaction of $Se \leftrightarrow CuSe \leftrightarrow Cu_3Se_2 \leftrightarrow Cu_{2-x}Se \leftrightarrow Cu_2Se$, with the reaction intermediates of CuSe, Cu_3Se_2 and $Cu_{2-x}Se$ being insoluble in aqueous electrolytes, minimizing the likelihood of ions shuttle effects, thus achieving a conspicuous specific capacity of 1350 mAh g_{Se}^{-1}. While zinc-selenium batteries remain an area of active research, further internal mechanisms and strategies remain to be explored.

Zinc-iodine batteries. Iodine is an attractive electroactive species with high natural abundance (55 μg L^{-1} of marine iodine) and low cost. In Zn//I_2 battery, iodine species undergo polymorphism redox conversion reactions (e.g., I_3^-, I^-, I^+, I_2, I^0, I_5^-) and a multi-electron transfer (e.g. two-electron transfer for I_2/I^- couple (0.54 V *vs.* SHE), four-electron transfer for I_2/I^+ couple (0.99 V *vs.* SHE)).[15, 23, 100] Theoretically, two-electron and four-electron transfers correspond to 211 and 422 mAh g^{-1} theoretical capacities, respectively.[26] However, there are several critical challenges faced by Zn//I_2 batteries (**Figure 6a**): (1) Limited effective electron transfer leading to a low operating platform and difficulty achieving high energy density. (2) Transformation and complexation of I_2 and I^- into highly soluble I_3^- during cycling, who can react with Zn and lead to self-discharge of the battery (known as "shuttle effect"); (3) Low utilization of redox pairs and sluggish kinetics of electrochemical reaction due to poor redox activity and concentration polarization.

In addition, the redox process of iodine entails the reversible conversion of solid and liquid states, and the conversion kinetics is controlled by the reactivity of active ions and ion/electron transport, as well as reaction reversibility. Given the poor conductivity and redox activity of iodine, the reversible conversion rate among iodine and iodide ions is pessimistic, while the concentration polarization of electrolyte hampers the transmission of active ions, thus causing sluggish electrolyte reaction kinetics. Therefore, corresponding optimization strategies are proposed:

Activation and promotion of redox pair conversion. To address the issue of inadequate capacity output resulting from poor iodine conductivity and activity, the commonly employed approach is to utilize porous carbon-based materials (e.g., carbon fiber, activated carbon, carbon nanotubes) as effective hosts for I_2, and incorporating heterogeneous atoms through doping.[101-106] The multi-level

hierarchical structure of functional electrodes facilitates the establishment of a stable solid-liquid interface, offering an efficient transmission path for the conversion process and promoting the electrocatalytic redox conversion process. Consequently, it greatly enhances the utilization of electrochemical redox active ions. An alternative strategy involves introducing Br^- to form I_2Br^- to stabilize iodine.[107] Generally, only two-thirds of the iodide ions contribute to the available capacity because the remaining one-third acts as complexing agents to stabilize free iodine, forming I_3^-. However, by employing Br^- to stabilize free iodine, preventing the capacity loss associated with the complexation of one-third of iodide ions can occur and then achieve full utilization of I^- (**Figure 6b**). Ultimately, the Zn//I_2 battery successfully achieved a remarkable energy density of 202 Wh L^{-1} in the catholyte. Notably, the agglomeration of solid I_2 frequently leads to channel blockage, especially in high energy density flow batteries. To address this issue, Xie et al.[108] designed a single pump configuration, with the pump positioned on the anode side, effectively mitigating battery failure stemming from I_2 clogging.

Multiple electron transfer is beneficial for achieving high energy density output. Compared to the 2e- conversion reaction of one redox couple (I^-/I_2), the 4e- consecutive conversion of multiple redox couples (I^-/I_2 and I_2/I^+) exhibits higher discharge platforms and larger capacity (**Figure 6c**).[26, 109] However, the conversion energy barrier of I_2/ I^- is high, leading to low reversibility and slow reaction kinetics, which results in low voltage and energy output. Additionally, the complexation product of I^- and I_2, I_3^-, easily undergoes oxidation at high concentrations to form I_2, with low reversibility yet, which reduces the utilization of active I^-. Hence, it is necessary to ensure that the I^-/I^+ system functions effectively as a redox active material to enhance its utilization during charge storage. Prompted by the inherent instability and hydrolytic susceptibility of I^+ species, the

investigators pursued the goal of enhancing the conversion probability of I_2/I^+ by incorporating Cl^- ions which exhibit high coordination affinity with I^+. Through the formation of the steadfast ICl compound, the hydrolysis of I^+ was effectively impeded.[26] This innovative approach proved successful in inducing a remarkable four-electron transfer process encompassing $I^-\rightarrow I^0\rightarrow I^+$, displaying significant advancements in the field.

Promoting ion/charge transfer to enhance kinetics. Slow ion/charge transfer is a crucial factor contributing to the low energy efficiency of batteries.[23] The diffusive limitations of ions primarily pertain to the transport of ions between electrodes. The diffusion polarization caused by concentration gradients, stemming from the discrepancy in ion concentration between the catholyte and anolyte significantly impacts the rate of ion diffusion, in addition with zinc and iodine ions possess larger size, resulting in greater transfer resistance.[110, 111] Hence, it becomes necessary to introduce supporting electrolytes with smaller dimensions to facilitate ion conduction. For instance, the introduction of smaller-sized NH_4^+ and H^+, or K^+ and Cl^- as supporting electrolytes is advantageous. [112, 113]These non-electrochemically active supporting ions can be transmitted between porous membranes, enabling rapid ion conduction **(Figure 6d)**. On the other hand, the diffusion rate of ions within electrode materials also affects the adsorption efficiency and charge-discharge efficiency. This necessitates a current collector with a higher specific surface area to provide ample ion diffusion channels and accessible active sites within the electrolyte.

Aiming at the issue of sluggish charge transfer of I_3^-/I^- conversion, it can be realized by introducing catalytically active sites into current collector (**Figure 6e**), which can enhance charge transfer and facilitate I_3^-/I^- conversion. Examples of such catalysts include MOFs and their derivatives with Lewis acidic metal catalytic centers,[103, 114] noble metal Pt,[115] MoC,[116] and tungsten disulfide[117,

[118]. Among them, defects such as sulfur vacancies, sulfur edges, and sulfur ligands in molybdenum disulfide serve as active sites for electrocatalysis, while their well-ordered morphology also improves the accessibility of the electrolyte, leading to excellent reaction kinetics.

Suppressing shuttle effect. Polyiodides tend to shuttle to the anode and react with zinc under concentration gradients and is accompanied by heat release, resulting in dissipating energy into the surrounding environment and causing capacity fading.[23] A common strategy to limit the shuttle of polyiodides is to use ion exchange membranes and hydrogels with function of immobilizing anionic chains, to restrict polyiodide shuttle and prevent electrolyte crossover.[119-121] Metal-organic frameworks (MOFs), a class of materials displaying adjustable pore sizes and remarkable order, frequently serve as ion screening materials, for the sake of modulating ion shuttling behavior and mitigating the detrimental effects of capacity fading associated with such behavior (**Figure 6f**).[122] Another strategy is to apply anode protection layers, such as employing a zeolite-based grinding method that replaces [SiO_4] tetrahedra in the zeolite lattice with [AlO_4] hexahedra, creating negatively charged lattice holes that allow the cationic Zn^{2+} to pass through but electrostatically repel the I_3^- anions.[123]

In addition to restricting the shuttle of polyiodides through separator, it is possible to immobilize I_2 in the cathode, such as applying adsorption site and interlayer adsorption.[124, 125] For instance, the $Co[Co_xFe_1@_x(CN)_6]$ material with ordered porosity and multiple catalytic active sites can serve as a host for I^-/I_2 storage and conversion, and the Co and Fe act as electrocatalytic sites to promote the conversion of I_2/I^- without generating I_3^-.[102] This strategy ultimately achieves excellent conversion kinetics and output capacity of 150.1 mAh g^{-1} at 4 A g^{-1} **(Figure 6g)**. Alternatively, a "double- layer (EDL)" electrode enables spontaneous formation of I_3^- at the interface between the conductive layer

and the adsorption layer during charging, followed by diffusion into the adsorption layer under the influence of concentration gradients. During discharging, I_3^- diffuses back to the interface, where it is reduced to I^-, thereby limiting I_3^- behavior.[126]

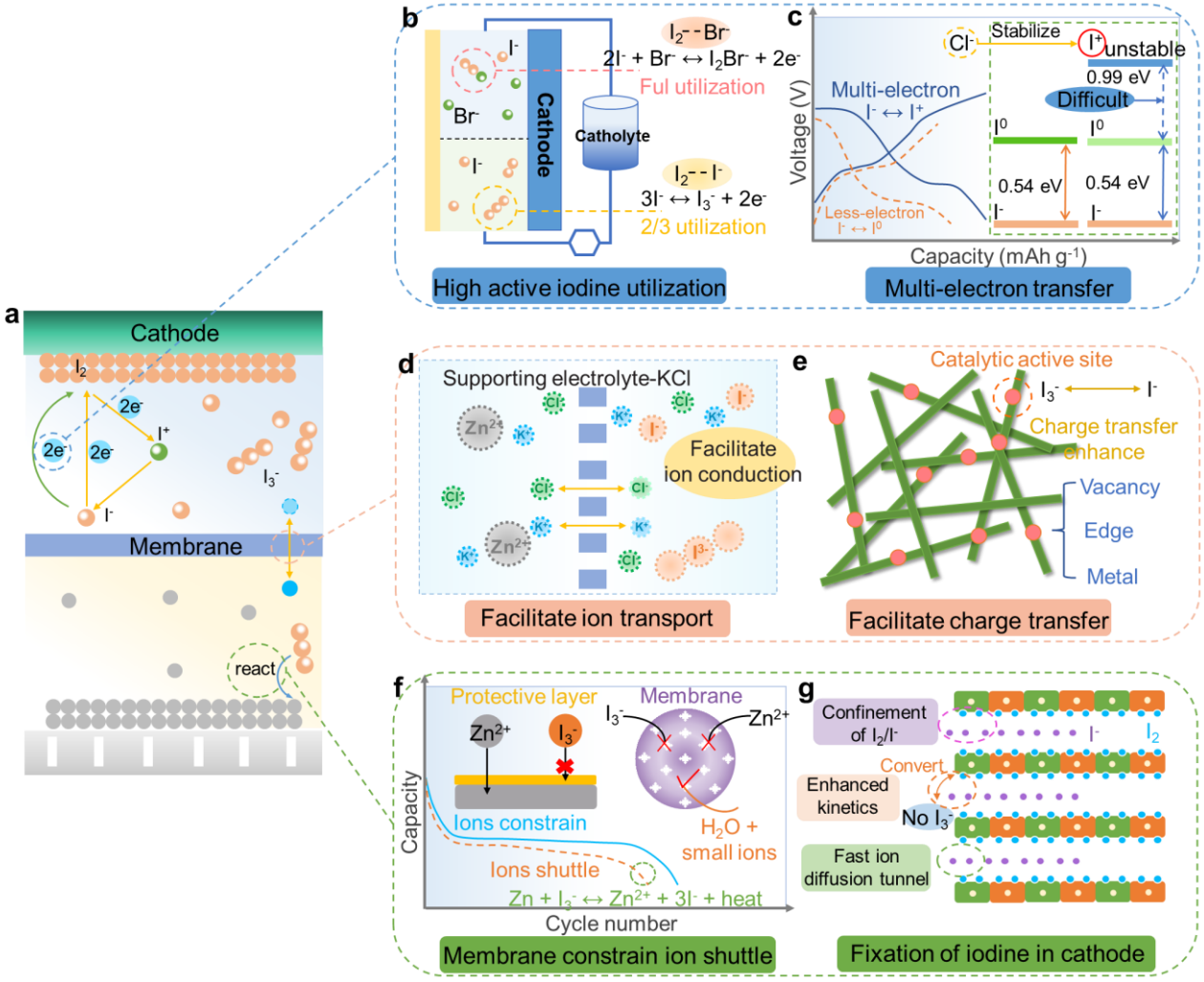

Figure 6. Reaction mechanism of zinc-iodine battery and corresponding optimization strategies. (a) Typical reaction mechanism of a zinc-iodine battery. (b) Improving the utilization of active iodine and (c) designing four-electron transfer to increase energy output. Improve conversion kinetics by promoting (d) ion transport and (e) charge transport. Mitigating the shuttle effect by (f) designing ion-selective membrane and anode protective layers and (g) confinement of iodide ions cathode materials.

Zinc-bromine batteries. Bromine is a promising cathode with high specific capacity of 335 mAh g^{-1} and Br_2/Br^- electrode potential of 1.06 V *vs.* SHE, as well as good solubility in aqueous electrolyte[16, 58]. Zn//Br_2 battery undergoes charge and discharge cycles through conversion reactions of Br_2 and its reduction products, with static and flow battery systems (**Figure 7a**). During the reduction process, Br undergoes reduction reactions with varying numbers of electrons and generate polybromide with different valence states (e.g., Br^-, Br_3^-, Br_5^-). The multivalent state of matter characterizes the possibility of designing batteries with multi-electron transfer.[127] Zn//Br_2 batteries are categorized into flow and flowless configurations, differing primarily in the inclusion of dual electrodes, electrolytes, and separators, while flow batteries necessitate additional sets of electrolytic reservoirs and pumps to maintain optimal levels of active ions (i.e., zinc ions and bromide ions) for efficient electrolyte flow.[17] The continuous supply of fresh electrolyte in this battery system effectively mitigates concentration polarization, thereby enhancing battery lifespan. However, this system demands higher capital investment and is more apt for large-scale energy storage applications.

It is worth mentioning that bromine and polybromide primarily exist in the liquid state under standard temperature and pressure conditions. The ionic state of bromine allows it to easily permeate the membrane, leading to undesired self-discharge and capacity degradation when it reacts with the zinc anode.[16, 128] Additionally, the corrosive nature and volatility of bromine can cause deterioration of the membrane and an elevation in internal air pressure, consequently reducing battery lifespan and potentially giving rise to hazardous incidents.[17] Moreover, bromine exhibits a sluggish conversion rate between Br_2 and Br^-, resulting in substantial polarization and diminished power density (**Figure 7b**).[129] To overcome these pressing challenges, the corresponding strategies have been proposed, encompassing: (1) Curtailing the shutting behavior exhibited by free bromine and polybromide

species; (2) Augmenting the kinetics of Br^-/Br_2 redox conversion.

Inhibits free bromide ion shuttling to reduce capacity fading (**Figure 7c**). Common strategies employed to restrict the presence of free bromine involve the development of cathodes with an abundant number of adsorption sites. Examples include cathodes with microporous electrodes containing protonated nitrogen-doped adsorption sites,[16] 2D MOFs/COFs cathode hosts,[129, 130] polymers cathode with an adsorbed function for polybromide,[128] and MXene loaded bromide ions.[131] Taking the MOF cathode host of 2D conjugated nickel polyphthalocyanine (NiPPc) as an example,[129] the porous structure facilitates a substantial bromine load, and the dense metal center, endowed with significant polarity, generates abundant adsorption sites for free bromine and bromide ions, thus achieves high capacity. Meanwhile, the π-π stacking layer structure of MOFs exhibit favorable carrier transport capabilities, while atomically dispersed Ni-N_4 sites can act as catalytically active sites, resulting in excellent conversion kinetics. Regarding electrolyte optimization, the implementation of gel/solid electrolytes serves to impede the movement of bromine and bromide ions, while simultaneously expanding the voltage range. However, the low ionic conductivity of them gives rise to high ohmic polarization and compromised charge transfer, consequently leading to sluggish reaction kinetics. Alternatively, the concept of incorporating complexing agents to immobilize bromide ions has emerged as a promising strategy. The commonly employed electrolyte is 2 M $ZnBr_2$, and the inclusion of bromine in a higher concentration of $ZnBr_2$ (7M) aids in augmenting the capacity. But the elevated levels of bromine elevate the likelihood of volatilization and corrosion, as well as ion crossover.[132] Complexing agents can effectively transform Br ions into a solid phase, which alleviates the above issues, and achieves a harmonious balance between $ZnBr_2$ concentration and bromine dissolution.[133, 134] As a result, excellent conversion kinetics and high capacity can be

achieved simultaneously. On the other hand, the ion exchange membrane plays a crucial role in obstructing the mobility of free bromine, yet the heightened resistance of membrane impedes the rate of ion exchange, thereby diminishing overall energy efficiency. To address this concern, recent studies have highlighted the capacity to attenuate ion exchange resistance through the manipulation of water cluster size within the membrane. [135]The broader channels provide ample space for efficient ion transportation, which facilitate its transportation rate. Additionally, the introduction of optimal functional layers, such as carbon layers, onto the membrane offers a means to alleviate the internal resistance encountered through promoting ion transmission, leading to outstanding reaction activity.[136]

Facilitates Br^-/Br_2 conversion to achieve high reaction kinetics (**Figure 7d**). To address the issue of sluggish Br_2/Br^- redox conversion, it is a prevalent approach to devise cathodes incorporating abundant catalytic active sites, such as metals and metal oxides (e.g., Pt, ZrO_x, TiO_x),[137, 138] heterogeneous element doping[16, 139] and active functional groups,[130] for the sake of promoting conversion rate. Alternatively, modulating the pH of the electrolyte, reactant concentration and supporting ions, or implementing a circulating electrolyte mechanism for alleviating concentration polarization and diminishing the internal resistance implicated in ion migration, in order to facilitating the conversion reaction.[127, 140, 141]

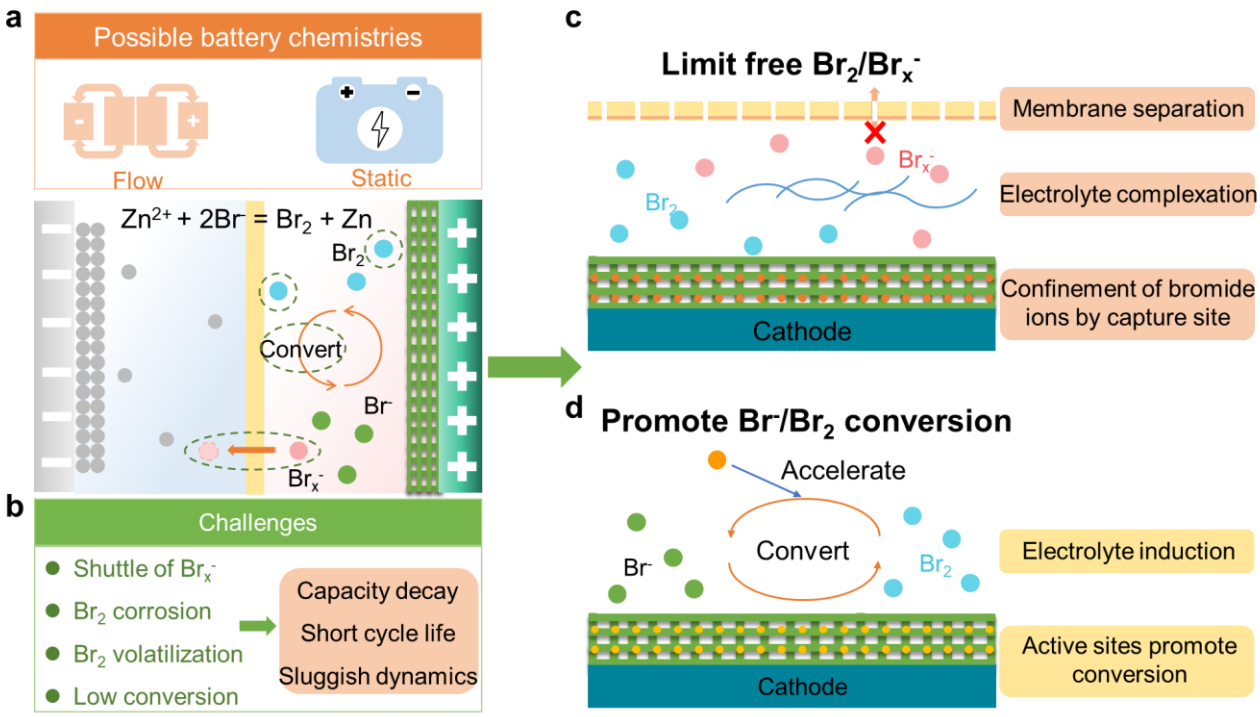

Figure 7. Reaction mechanism, challenges and optimization strategies of zinc-bromine batteries. (a) Types and reaction mechanisms of zinc-bromine batteries and (b) encountered challenges. Strategies to (c) limit free bromine and (d) promote Br^-/Br_2 conversion.

Other conversion-type batteries. Typical Zn-Cu batteries and Zn-Fe batteries also belong to conversion-type battery. Among them, Zn-Cu battery (also called Daniel batteries) has a high theoretical capacity of 844 mAh g^{-1} based on two-electron transfer ($Cu^0 \leftrightarrow Cu^{2+}$).[18, 29, 142] Zinc-copper batteries contain no rare earths or toxic materials and can directly recyclable, which is attractive. Traditional Zn-Cu battery is a primary battery with Zn as anode and Cu as cathode, along with sulfuric acid, zinc sulfate or copper sulfate as electrolytes. Due to the greater reactivity of Zn compared to Cu, a potential difference exists, resulting in the oxidation reaction at the anode and the reduction reaction at the cathode, along with battery cycle achievement.

$$2H^+ + 2e^- \rightarrow H_2 \text{ and } Cu^{2+} + 2e^- \rightarrow 2Cu \quad (19)$$

Zn^{2+} and Cu^{2+} entail an irreversible displacement reaction in an acidic solution, rendering the

battery non-rechargeable. A key prerequisite for building rechargeable Zn-Cu battery is to avoid crossover of zinc and copper ions to achieve reaction reversibility. Copper and its oxides like $Cu(OH)_2$, CuO, and Cu_2O are highly insoluble in alkaline electrolytes, and the researchers designed an alkaline Zn-Cu battery to achieve reversible cycling through reversible redox between Cu and $Cu(OH)_2$/CuO (**Equation 20**)[29].

$$Zn + Cu(OH)_2/CuO = Zn(OH)_2/ZnO + Cu \qquad (20)$$

Nevertheless, the efficacy of the aforementioned approach is compromised by its suboptimal conversion efficiency and limited reversibility, along with severe corrosion of zinc anode in alkaline electrolyte, leading to a short battery cycle life. Addressing these issues, He et al.[143] report an anion exchange membrane (AEM) that can alleviate the ions crossover between Zn and Cu ions, thereby facilitating the reversible conversion of Zn and Cu, ultimately allowing for a standardized 1.1 V output voltage. Alternatively, an alternative solution is proposed involving the design of an organic-aqueous two-phase electrolyte. The unique composition ensures the confinement of Cu ions within a hydrated state in the aqueous phase, and chloride ions act as charge carriers between the two phases to maintain electrical neutrality, which can also prevent ions crossover.[144]

Zn-Fe batteries involve liquid-phase reactions that enable capacity output by means of the redox conversion of active ions.[145-147] In order to enhance energy output, the flow system with functions of distinct catholyte and anolyte, and constantly updated electrolytes are typically employed to achieve optimal redox potentials for the respective electrodes. Therefore, affordable, low-resistance, and highly stable membrane with the properties of facilitating rapid ion exchange are expected. Chang et al.[148] introduced a cost-effective sulfonated polyetheretherketone (SPEEK-K) membrane, with notable characteristics such as high swelling rate, minimal resistance and high stability, which costs

only one-thirteenth of the commercially available Nafion 117 film. Meanwhile, a double-membrane three-electrolyte chamber are also reported, incorporating Na^+ and Cl^- in the neutral electrolyte chamber situated in the middle to serve as supporting ions for charge balancing.[147] This configuration can mitigate the issue of ion crossover, leading to improved ion transmission rates and, subsequently, enhanced energy efficiency. Alternatively, one could initiate the exploration by focusing on electrochemical reactions and developing redox couples with higher potential differentials. Zn-Fe flow batteries can operate over a wide pH range, while redox pairs under different environment are studied for the sake of high voltage output, such as $Fe(CN)_6^{3-}/Fe(CN)_6^{4-}$, 0.36 V *vs.* SHE, Fe^{3+}/Fe^{4+}, 0.77 V *vs.* SHE, $[Fe(glycine)_2]^{3+}/[Fe(glycine)_2]^{2+}$, 0.51 V *vs.* SHE, for the sake of high voltage output.[19, 149, 150] In addition, the Zn-Te battery has garnered recent interest as a conversion-type battery, operating via a two-step reversible conversion reaction of Te to $ZnTe_2$ and $ZnTe_2$ to ZnTe for charge and discharge processes. [151] Notably, both the intermediate species $ZnTe_2$ and the end-product ZnTe exhibit insolubility in aqueous environments, circumventing the conventional challenges associated with the "shuttle effect" in zinc-chalcogen battery systems.

Table 2. Summary of conversion-type zinc battery performances.

Battery type	Reaction mechanism	Electrolyte	Current density	Average voltage	Practical capacity	Ref.
Zn//MnO_2 battery	$Zn^{2+} + Mn^{2+} + 2H_2O \leftrightarrow Zn + MnO_2 + 4H^+$	1 M $ZnSO_4$ + 1 M $MnSO_4$ + 0.1 M H_2SO_4	2 mA cm^{-2}	1.95 V	570 mAh g^{-1}	9
Zn//MnO_2 battery	$Mn^{2+} + 2H_2O + Zn^{2+} \leftrightarrow MnO_2 + 4H^+ + Zn$	1 M $Zn(CH_3COO)_2$ + 0.4 M $Mn(CH_3COO)_2$	5 mA cm^{-2}	1.5 V	556 mAh g^{-1}	81
Zn//MnO_2 flow battery	$2MnAc_2 + 2H_2O\text{-}2e^- \leftrightarrow MnO_2 + 4HAc + Mn^{2+}$	0.5 M $Mn(Ac)_2$ + 0.5 M $Zn(Ac)_2$ + 2 M KCl	40 mA cm^{-2}	1.55 V	13.3 ,mAh cm^{-1}	86

Zn//S@Fe-PANi battery	$S_8 + Zn_2Fe^{II}(CN)_6 \leftrightarrow ZnS + Zn_{1.5}Fe^{III}(CN)_6$	2 M $ZnSO_4$	200 mA g^{-1}	0.58 V	1205 mAh g^{-1}	152
Zn//S@C battery	$S + 2Cu^{2+} + 2Zn \leftrightarrow Cu_2S + 2Zn^{2+}$	0.5 M $ZnSO_4$ + 0.5 M $CuSO_4$	3.5 mg cm^{-2}	1.15 V	2063 mAh g_s^{1}	28
Zn//S@C battery	$S + 2Cu^{2+} + 2Zn \rightarrow Cu_2S + 2Zn^{2+}$ $Cu^{2+} + xO_2 + Zn \rightarrow (1-4x)Cu + 2xCu_2O + Zn^{2+}$	Catholyte: 0.5 M $CuSO_4$; Anolyte: 0.5 M $ZnSO_4$	0.1 mA cm^{-2}	0.99 V	48 mAh cm^{-2}	92
Zn//Se battery	$Se + Zn \leftrightarrow ZnSe$	1 M $ZnSO_4$	0.1 A g^{-1}	0.61 V	611 mAh g_{Se}^{-1}	13
Zn//I_2 battery	$Zn^{2+} + 2I^- \leftrightarrow Zn + I_2$ $Zn^{2+} + I_2 + 2\,Cl^- \leftrightarrow Zn + 2\,ICl$	$ZnCl_2$: LiCl : CH_3CN = 19:19:8	400 mA g^{-1}	1.26 V	594 mAh g^{-1}	26
Zn//TiC_2I_2 battery	$Zn^{2+} + 2I^- \leftrightarrow Zn + I_2$ $Zn^{2+} + I_2 \leftrightarrow Zn + 2\,I^+$	2 M $ZnCl_2$ + 1 M KCl	500 mA g^{-1}	1.35 V	207 mAh g^{-1}	153
Zn//I_2 battery	$Zn^{2+} + 3I^- \leftrightarrow Zn + I_3^-$	2 M $ZnSO_4$	160 mA g^{-1}	1.17 V	201.27 mAh g^{-1}	122
Zn//Br_2 battery	$2Br^- \leftrightarrow Br_2 + 2e^-$ $Br_2 + Br_n^-$ (n=1,3,5…) $\leftrightarrow Br_{n+2}^-$	2.25 M $ZnBr_2$	5 mA cm^{-2}	1.65 V	5 mAh cm^{-2}	16
Zn//Br_2 battery	$Zn + 4KOH + Br_2 \leftrightarrow K_2[Zn(OH)_4] + 2KBr$	Anolyte: 6 M KOH; Catholyte: 0.1 M Br_2 + 1 M KBr + 5 M CH_3COOK	2 A g^{-1}	2.15 V	378 mAh g^{-1}	154
Zn//Cu battery	$Zn + Cu(OH)_2/CuO \leftrightarrow Zn(OH)_2/ZnO + Cu$	1 M $ZnSO_4$ + 1 M KOH	0.1 A g^{-1}	0.76 V	718 mAh g^{-1}	29
Zn//Fe flow battery	$Zn + 4OH^- + 2Fe^{3+} \leftrightarrow 2Fe^{2+} + Zn(OH)_4^{2-}$	Anolyte: 0.4 M $Zn(OH)_4^{2-}$ + 3 M NaOH Catholyte: 0.8 M $Na_4Fe(CN)_6$ + 3 M KOH	840 mA cm^{-2}	1.3 V		146

Conclusions and perspectives

In this review, we have highlighted the fundamental scientific understanding, especially in terms

of thermodynamics and kinetics, of conversion reactions in AZBs. Deep insights have been achieved in the areas of conversion reaction mechanisms, challenges, as well as the corresponding perspectives. These conversion reactions include Zn metal or Zn compound-based conversion reaction, manganese-based conversion reaction, chalcogenide-based conversion reaction, halogen-based conversion reaction, copper, or iron-based conversion reaction, with the performances shown as **Table 2**. It is no doubt that the conversion-type AZBs remain far from maturity. In many of these areas, their common challenges (e.g., ion shuttle leading to self-discharge; restricted electron transfer limiting energy output; sluggish conversion rate; side reactions affecting performance) and the common optimized strategies proposed by the researchers (e.g., advanced configuration; continuous conversion; effective membrane; electrolyte regulation; functional cathodes) are summarized in **Figure 8**. Although these strategies have been proposed, a comprehensive understanding of the thermodynamics and kinetics, which lays the core for conversion reaction, is still lacking. To better understand and design these conversion reactions, we provide a systematic discussion of thermodynamics and kinetics as following:

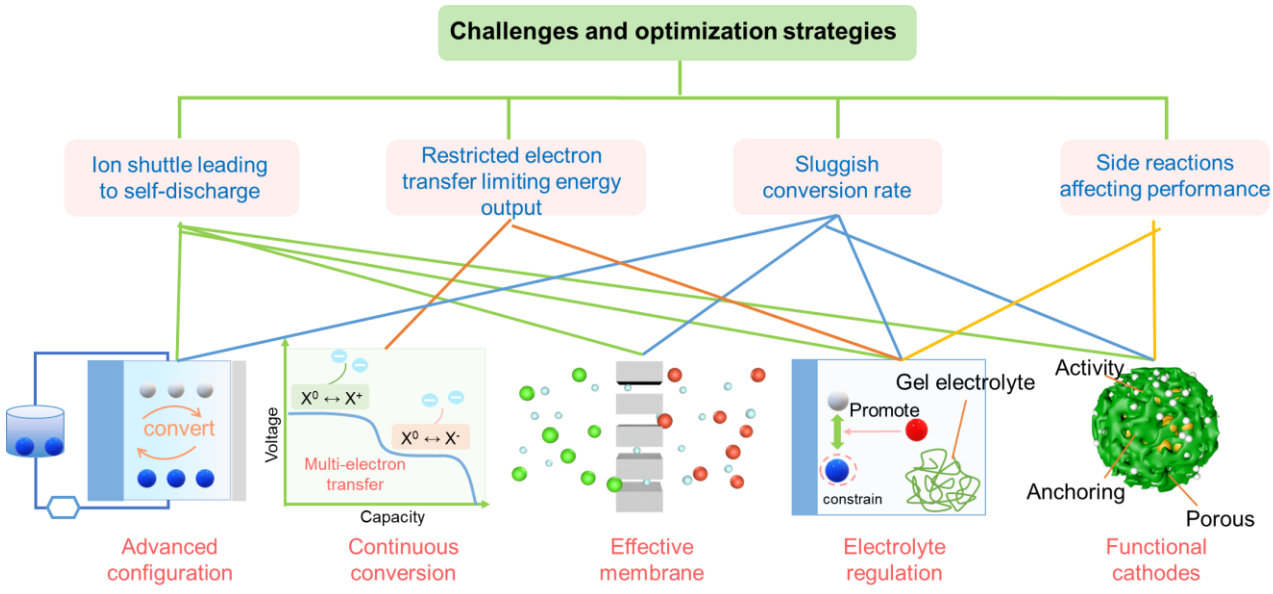

Figure 8. Summary of challenges faced by conversion-type batteries and optimization strategies.

Thermodynamics behaviors of conversion-type AZBs. Thermodynamic aspects include the working potential, capacity, stability, and reversibility of the conversion reaction (**Figure 9a**). The energy output depends on the molar mass (M) of the electrode pair, electrode potential (E), and effective transferred electrons (n). The multiple electron transfer is an effective strategy for increasing the energy output of batteries, such as from two electrons to four electrons in zinc-iodine batteries, since they can activate redox pairs located at high potential while contributing a large capacity. The pursuit of high energy output, however, will inevitably cause instability of the battery system. A stable thermodynamic process during multiple electron transfer can be achieved by designing cascade reactions,[26, 92, 109] developing new reaction route,[9] or introducing additional redox pairs.[88] Cascading reactions require activation of new redox pairs, however, newly activated redox pairs (reaction intermediates) are often difficult to stabilize, requiring the introduction of additives for complexation like Cl^-.[26, 109] Introducing additional redox pair is another strategy to utilize ion carriers as an additional reservoir of electron charge to fully exploit the redox potential and achieve a multi-electron reaction.[91]

In addition to the stability of the reaction intermediates, the electrode stability and reversibility are extremely important for these conversion reactions, which affect the coulombic efficiency (CE) and energy efficiency (EE) of batteries. Dendrite growth, hydrogen evolution and corrosion are recognized as the main factors affecting the stability and reversibility of Zn anode, thus deteriorate the CE of the Zn-based batteries. For solid phase reaction (**Figure 9c**), the stability of electrode is mainly affected by the reversibility of the conversion products. For example, the conversion of Mn^{2+}//MnO_2, S//ZnS and Se//ZnSe, while the reaction reversibility is affected by electrode conductivity and passivation products such as “dead” Mn and inactive sulfides. It is similar to the

solid to solid conversion of zinc anode. The reversibility of reaction is limited by the activity of the reactants ($2ZnCO_3 \cdot 3Zn(OH)_2$ and Zn) and the accumulation of by-products. For liquid phase reaction (**Figure 9d**), the stability suffers from the current collector and active sites, charge transfer/diffusion coefficient of liquid reactant, shuttle effect and consumption of active ions; etc. In many cases, an important indicator, e.g., EE, is easy to be overlooked, which is not good in many conversion reactions in spite to their excellent stability, especially in solid phase reaction, such as Zn//S and Zn//Se battery. The energy efficiency are influenced by various factors, including electrochemical polarization, concentration polarization, electrochemical reactivity, and competition from side reactions. Polarization also affects the solid-liquid conversion of zinc anode, especially the aggregation of Zn^{2+} tips under the influence of diffusion polarization is the main cause of zinc dendrites. In addition, the electrochemically stabilized voltage window of aqueous electrolytes, which is determined by the electrolyte composition and its compatibility with electrode, plays an important role in the stability and reversibility of the conversion reaction. Therefore, more attention needs to be paid to the stability of the electrolyte, especially the design of multi-electron transfer and high-voltage conversion reactions.

Kinetics behaviors of conversion-type AZBs. Factors influencing the kinetics of conversion reactions primarily include charge transfer resistance, diffusion rates, and phase transition energy barriers (**Figure 9b**). Charge transfer resistance refers to the transfer resistance between electrodes and electrolytes. Effective strategies for reducing charge transfer resistance involve designing highly porous electrodes with large specific surface areas to facilitate rapid ion migration and reaction (e.g., Mxene, porous carbon), optimizing the ion conductivity and viscosity of the electrolyte to promote faster charge transfer, and designing well-defined and stable interfaces to enhance interface reactions

(e.g., MOFs/COFs, polymer coating). The diffusion rate is quantified through diffusion coefficients, and the diffusion coefficient of cations at the interface can be calculated[155]:

$$D = 0.5(\frac{RT}{An^2F^2\sigma_\omega C})^2 \quad (21)$$

R represents a constant, T denotes temperature, A signifies the surface area of the electrode, n represents the number of electrons per molecule in the reduction process. σ_ω represents the Warburg factor and C denotes the concentration of ions. According to the **Equation 21**, it can be observed that the diffusion coefficient is primarily influenced by the number of transfer electrons, ions concentration, electrode specific surface area, and activation temperature. On the other hand, since conversion reactions predominantly involve electron transfer through phase transitions, the magnitude of the phase transition energy barrier determines the rate of the reaction. The bond energy of chemical bonds plays a crucial role in determining the kinetic performance.[96] Solid phase reactions require overcoming high energy barriers due to the stable chemical bonds of solid reactant, as well as overcome the low electronic conductivity of most solid phases (**Figure 9c**). Rapid bond breaking and formation are crucial for achieving high-rate performance, and the interfacial characteristics of electrodes/electrolytes and solid phase conductivity significantly impact ions/electrons transfer, which in turn affects reaction efficiency. Hence, a porous and highly active functional cathode should be desired, such as S@CNTs, $Co[Co_xFe_1@_x(CN)_6]$, 2D NiPPC. On the contrary, liquid phase reactions by ionic conversion exhibits lower energy barriers and excellent kinetics, and the capacity is determined by the composition and concentration of the electrolyte (**Figure 9d**). Charge transfer resistance and diffusion coefficients are mainly influenced by factors such as electrolyte composition, temperature, polarization, solubility of active ions, flow rate, and electrode specific surface area. Given the characteristics of liquid phase reactions, decoupled flow batteries with advantages of

electrolyte separation and elimination of concentration polarization are favored. On the other hand, as the current collector serves as a carrier for active sites in redox reactions, its physicochemical properties play a critical role in battery kinetics, including catalytic activity, porosity, hydrophilicity, and electronic conductivity. Additionally, the conductivity and wettability of the electrode/electrolyte interface can influence the phase conversion reaction.[156]

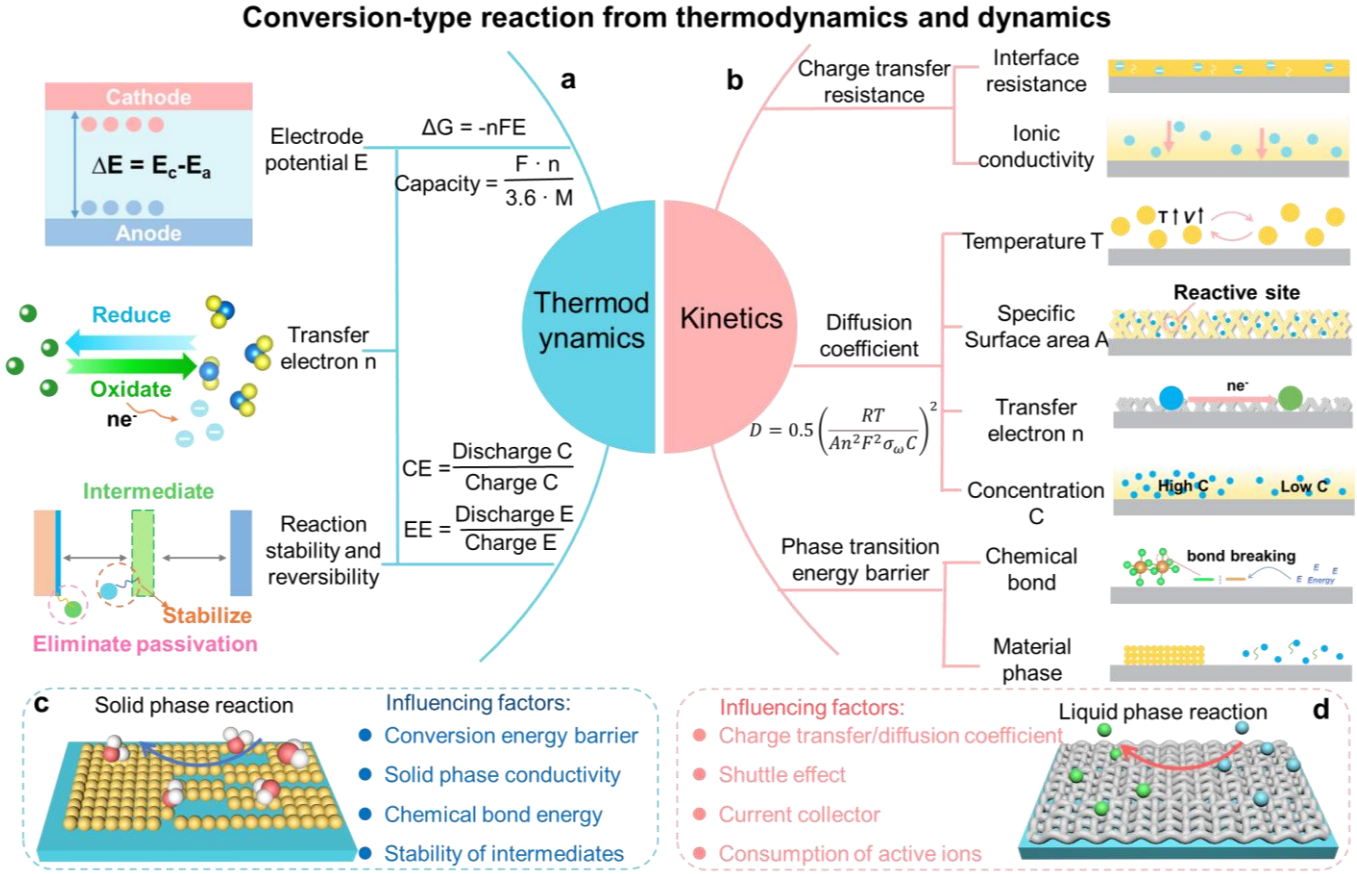

Figure 9. A schematic discussion of the influencing factors on the (a) thermodynamics and (b) kinetics of conversion-type AZBs. Summary of influencing factors of (c) solid phase reaction and (d) liquid phase reaction.

AUTHOR INFOR MATION

Corresponding Authors

Xuefang Xie — College of Physical Science and Technology, Xinjiang University, Urumqi 830017, Xinjiang, P.R. China; orcid.org/0000-0003-0663-7232; Email: xiexuefang@xju.edu.cn

Wai-Yeung Wong — Department of Applied Biology & Chemical Technology and Research Institute for Smart Energy, The Hong Kong Polytechnic University, Hong Kong, P.R. China; orcid.org/0000-0002-9949-7525; Email: wai-yeung.wong@polyu.edu.hk

Guozhao Fang — National Energy Metal Resources and New Materials Key Laboratory, Central South University, Changsha 410083, P.R. China**;** orcid.org/ 0000-0003-2140-0145**;** Email: fg_zhao@csu.edu.cn

Authors

Xianhong Chen — Department of Applied Biology & Chemical Technology, The Hong Kong Polytechnic University, Hong Kong, P.R. China

Pengchao Ruan — School of Materials Science and Engineering, Hunan Provincial Key Laboratory of Electronic Packaging and Advanced Functional Materials, Central South University, Changsha 410083, China

Shuquan Liang — National Energy Metal Resources and New Materials Key Laboratory, Central South University, Changsha 410083, P.R. China; orcid.org/ 0000-0003-2140-0145

Notes

The authors declare no competing financial interest.

Biographies

Xianhong Chen received her B.S degree from Central South University in 2022. Now she is a Ph.D. student at Department of Applied Biology & Chemical Technology, The Hong Kong Polytechnic University.

Xuefang Xie received her Ph.D. degree from Central South University in 2021. After graduation, she joined Xinjiang University as an associate professor.

Pengchao Ruan is working as a master student at School of Materials Science and Engineering, Central South University.

Shuquan Liang has been the Dean of School of Materials Science and Engineering in Central South University since 2010. He is the winner of the Monash University Engineering Sir John Medal.

Wai-Yeung Wong is the Dean of Faculty of Science and a Chair Professor of Chemical Technology at The Hong Kong Polytechnic University. He was elected as the Foreign Member of the European Academy of Sciences in 2023.

Guozhao Fang received his Ph.D. degree (2019) from *Central South University*. After graduation, he joined *Central South University* as a professor. His research interests mainly focus on the low-cost energy storage of aqueous zinc-ion batteries and sodium-ion batteries, especially in electrolyte and electrolyte/electrode interfaces.

Acknowledgements

G.Z. F. thanks the National Natural Science Foundation of China (Grant no. 52072411, 51932011, 52272260), the science and technology innovation Program of Hunan Province (Grant no. 2021RC3001), Central South University Innovation-Driven Research Programme (Grant No. 2023CXQD038). W.-Y. W. thanks the RGC Senior Research Fellowship Scheme (SRFS2021-5S01),

Research Institute for Smart Energy (CDAQ) and Miss Clarea Au for the Endowed Professorship in Energy (847S) for the financial support. X.F. X. thanks the Natural Science Foundation of Xinjiang Uygur Autonomous Region (Grant No. 2023D01C168), Autonomous Region "Tianchi Talent" Introduction Program Youth Doctoral Program (Grant No. 51052300577).

References:

1. Liu, Y.; Lu, X.; Lai, F.; Liu, T.; Shearing, P. R.; Parkin, I. P.; He, G.; Brett, D. J. L., Rechargeable aqueous Zn-based energy storage devices. *Joule* **2021,** *5* (11), 2845-2903.
2. Wan, F.; Zhou, X.; Lu, Y.; Niu, Z.; Chen, J., Energy Storage Chemistry in Aqueous Zinc Metal Batteries. *ACS Energy Lett.* **2020,** *5* (11), 3569-3590.
3. Gao, X.; Dai, Y.; Zhang, C.; Zhang, Y.; Zong, W.; Zhang, W.; Chen, R.; Zhu, J.; Hu, X.; Wang, M.; Chen, R.; Du, Z.; Guo, F.; Dong, H.; Liu, Y.; He, H.; Zhao, S.; Zhao, F.; Li, J.; Parkin, I. P.; Carmalt, C. J.; He, G., When It's Heavier: Interfacial and Solvation Chemistry of Isotopes in Aqueous Electrolytes for Zn-ion Batteries. *Angew. Chem. Int. Ed.* **2023,** *62* (16), e202300608.
4. Ma, L.; Schroeder, M. A.; Borodin, O.; Pollard, T. P.; Ding, M. S.; Wang, C.; Xu, K., Realizing high zinc reversibility in rechargeable batteries. *Nat. Energy* **2020,** *5* (10), 743-749.
5. Dou, X.; Xie, X.; Liang, S.; Fang, G., Low-current-density stability of vanadium-based cathodes for aqueous zinc-ion batteries. *Sci Bull.* **2024,** *50*, 21-46.
6. Zhang, T.; Chen, Q.; Li, X.; Liu, J.; Zhou, W.; Wang, B.; Zhao, Z.; Li, W.; Chao, D.; Zhao, D., Redox Mediator Chemistry Regulated Aqueous Batteries: Insights into Mechanisms and Prospects. *CCS Chemistry* **2022,** *4* (9), 2874-2887.
7. Li, W.; Wang, D., Conversion-type Cathode Materials for Aqueous Zn Metal Batteries in Non-Alkaline Aqueous Electrolytes: Progress, Challenges, and Solutions. *Adv. Mater.* **2023**, DOI: 10.1002/adma.202304983.
8. Ruan, P.; Liang, S.; Lu, B.; Fan, H. J.; Zhou, J., Design Strategies for High-Energy-Density Aqueous Zinc Batteries. *Angew. Chem. Int. Ed.* **2022,** *61* (17), e202200598.
9. Chao, D.; Zhou, W.; Ye, C.; Zhang, Q.; Chen, Y.; Gu, L.; Davey, K.; Qiao, S. Z., An Electrolytic Zn-MnO(2) Battery for High-Voltage and Scalable Energy Storage. *Angew. Chem. Int. Ed.* **2019,** *58* (23), 7823-7828.
10. Zhang, X.; Zhang, B.; Yang, J. L.; Wu, J.; Jiang, H.; Du, F.; Fan, H. J., High-Sulfur Loading and Single Ion-Selective Membranes for High-Energy and Durable Decoupled Aqueous Batteries. *Adv. Mater.* **2023,** *36* (3), e2307298.
11. Liu, J.; Zhou, W.; Zhao, R.; Yang, Z.; Li, W.; Chao, D.; Qiao, S. Z.; Zhao, D., Sulfur-Based Aqueous Batteries: Electrochemistry and Strategies. *J. Am. Chem. Soc.* **2021,** *143* (38), 15475-15489.
12. Dai, C.; Hu, L.; Chen, H.; Jin, X.; Han, Y.; Wang, Y.; Li, X.; Zhang, X.; Song, L.; Xu, M.; Cheng, H.; Zhao, Y.; Zhang, Z.; Liu, F.; Qu, L., Enabling fast-charging selenium-based aqueous batteries via conversion reaction with copper ions. *Nat Commun* **2022,** *13* (1), 1863.
13. Chen, Z.; Mo, F.; Wang, T.; Yang, Q.; Huang, Z.; Wang, D.; Liang, G.; Chen, A.; Li, Q.; Guo, Y.; Li, X.; Fan, J.; Zhi, C., Zinc/selenium conversion battery: a system highly compatible with both organic and aqueous electrolytes. *Energy Environ. Sci.* **2021,** *14* (4), 2441-2450.

14. Yang, Y.; Liang, S.; Lu, B.; Zhou, J., Eutectic electrolyte based on N-methylacetamide for highly reversible zinc–iodine battery. *Energy Environ. Sci.* **2022,** *15* (3), 1192-1200.
15. Ma, J.; Liu, M.; He, Y.; Zhang, J., Iodine Redox Chemistry in Rechargeable Batteries. *Angew. Chem. Int. Ed.* **2021,** *60* (23), 12636-12647.
16. Lee, J. H.; Byun, Y.; Jeong, G. H.; Choi, C.; Kwen, J.; Kim, R.; Kim, I. H.; Kim, S. O.; Kim, H. T., High-Energy Efficiency Membraneless Flowless Zn-Br Battery: Utilizing the Electrochemical-Chemical Growth of Polybromides. *Adv. Mater.* **2019,** *31* (52), e1904524.
17. Mahmood, A.; Zheng, Z.; Chen, Y., Zinc-Bromine Batteries: Challenges, Prospective Solutions, and Future. *Adv Sci (Weinh)* **2023,** *11* (3), e2305561.
18. Schorr, N. B.; Arnot, D. J.; Bruck, A. M.; Duay, J.; Kelly, M.; Habing, R. L.; Ricketts, L. S.; Vigil, J. A.; Gallaway, J. W.; Lambert, T. N., Rechargeable Alkaline Zinc/Copper Oxide Batteries. *ACS Appl. Energy Mater.* **2021,** *4* (7), 7073-7082.
19. Xie, C.; Duan, Y.; Xu, W.; Zhang, H.; Li, X., A Low-Cost Neutral Zinc-Iron Flow Battery with High Energy Density for Stationary Energy Storage. *Angew. Chem. Int. Ed.* **2017,** *56* (47), 14953-14957.
20. Liu, Z.; Li, L.; Qin, L.; Guo, S.; Fang, G.; Luo, Z.; Liang, S., Balanced Interfacial Ion Concentration and Migration Steric Hindrance Promoting High-Efficiency Deposition/Dissolution Battery Chemistry. *Adv. Mater.* **2022,** *34* (40), e2204681.
21. Huang, Y. X.; Wu, F.; Chen, R. J., Thermodynamic analysis and kinetic optimization of high-energy batteries based on multi-electron reactions. *Natl Sci Rev* **2020,** *7* (8), 1367-1386.
22. Zhao, Y.; Wang, D.; Li, X.; Yang, Q.; Guo, Y.; Mo, F.; Li, Q.; Peng, C.; Li, H.; Zhi, C., Initiating a Reversible Aqueous Zn/Sulfur Battery through a "Liquid Film". *Adv. Mater.* **2020,** *32* (32), 2003070.
23. Lin, D.; Li, Y., Recent Advances of Aqueous Rechargeable Zinc-Iodine Batteries: Challenges, Solutions, and Prospects. *Adv. Mater.* **2022,** *34* (23), e2108856.
24. Xu, H.; Yang, W.; Li, M.; Liu, H.; Gong, S.; Zhao, F.; Li, C.; Qi, J.; Wang, H.; Peng, W.; Liu, J., Advances in Aqueous Zinc Ion Batteries based on Conversion Mechanism: Challenges, Strategies, and Prospects. *Small* **2024**, DOI: 10.1002/smll.202310972.
25. Kang, J.; Zhao, Z.; Li, H.; Meng, Y.; Hu, B.; Lu, H., An overview of aqueous zinc-ion batteries based on conversion-type cathodes. *Energy Materials* **2022,** *2*, 200009.
26. Zou, Y.; Liu, T.; Du, Q.; Li, Y.; Yi, H.; Zhou, X.; Li, Z.; Gao, L.; Zhang, L.; Liang, X., A four-electron Zn-I(2) aqueous battery enabled by reversible I(-)/I(2)/I(+) conversion. *Nat Commun* **2021,** *12* (1), 170.
27. Li, W.; Wang, K.; Jiang, K., A Low Cost Aqueous Zn–S Battery Realizing Ultrahigh Energy Density. *Adv. Sci.* **2020,** *7* (23), 2000761.
28. Dai, C.; Jin, X.; Ma, H.; Hu, L.; Sun, G.; Chen, H.; Yang, Q.; Xu, M.; Liu, Q.; Xiao, Y.; Zhang, X.; Yang, H.; Guo, Q.; Zhang, Z.; Qu, L., Maximizing Energy Storage of Flexible Aqueous Batteries through Decoupling Charge Carriers. *Adv. Energy Mater.* **2021,** *11* (14), 2003982.
29. Zhu, Q.; Cheng, M.; Zhang, B.; Jin, K.; Chen, S.; Ren, Z.; Yu, Y., Realizing a Rechargeable High-Performance Cu–Zn Battery by Adjusting the Solubility of Cu^{2+}. *Adv. Funct. Mater.* **2019,** *29* (50), 1905979.
30. Ma, L.; Chen, S.; Long, C.; Li, X.; Zhao, Y.; Liu, Z.; Huang, Z.; Dong, B.; Zapien, J. A.; Zhi, C., Achieving High-Voltage and High-Capacity Aqueous Rechargeable Zinc Ion Battery by Incorporating Two-Species Redox Reaction. *Adv. Energy Mater.* **2019,** *9* (45), 1902446.
31. Yang, Q.; Li, Q.; Liu, Z.; Wang, D.; Guo, Y.; Li, X.; Tang, Y.; Li, H.; Dong, B.; Zhi, C., Dendrites in Zn-Based Batteries. *Adv. Mater.* **2020,** *32* (48), e2001854.
32. Wu, S.; Hu, Z.; He, P.; Ren, L.; Huang, J.; Luo, J., Crystallographic engineering of Zn anodes for aqueous batteries. *eScience* **2023,** *3* (3), 100120.

33. Hou, Z.; Zhang, T.; Liu, X.; Xu, Z.; Liu, J.; Zhou, W.; Qian, Y.; Fan, H. J.; Chao, D.; Zhao, D., A solid-to-solid metallic conversion electrochemistry toward 91% zinc utilization for sustainable aqueous batteries. *Sci. Adv.* **2022,** *8* (41), eabp8960.
34. Zhang, Q.; Luan, J.; Tang, Y.; Ji, X.; Wang, H., Interfacial Design of Dendrite-Free Zinc Anodes for Aqueous Zinc-Ion Batteries. *Angew. Chem. Int. Ed.* **2020,** *59* (32), 13180-13191.
35. Luo, X.; Zhou, M.; Luo, Z.; Shi, T.; Li, L.; Xie, X.; Sun, Y.; Cao, X.; Long, M.; Liang, S.; Fang, G., Regulation of desolvation process and dense electrocrystalization behavior for stable Zn metal anode. *Energy Storage Materials* **2023,** *57*, 628-638.
36. Jin, S.; Chen, P. Y.; Qiu, Y.; Zhang, Z.; Hong, S.; Joo, Y. L.; Yang, R.; Archer, L. A., Zwitterionic Polymer Gradient Interphases for Reversible Zinc Electrochemistry in Aqueous Alkaline Electrolytes. *J. Am. Chem. Soc.* **2022,** *144* (42), 19344-19352.
37. Zhang, Y.; Wu, Y.; Ding, H.; Yan, Y.; Zhou, Z.; Ding, Y.; Liu, N., Sealing ZnO nanorods for deeply rechargeable high-energy aqueous battery anodes. *Nano Energy* **2018,** *53*, 666-674.
38. Li, L.; Tsang, Y. C. A.; Xiao, D.; Zhu, G.; Zhi, C.; Chen, Q., Phase-transition tailored nanoporous zinc metal electrodes for rechargeable alkaline zinc-nickel oxide hydroxide and zinc-air batteries. *Nat Commun* **2022,** *13* (1), 2870.
39. Wu, W.; Yang, X.; Wang, K.; Lin, Z.; Shi, H. Y.; Sun, X., Inducing the Solid–Liquid Conversion of Zinc Metal Anode in Alkaline Electrolytes by a Complexing Agent. *Adv. Funct. Mater.* **2022,** *32* (45), 2207397.
40. Mu, Y.; Li, Z.; Wu, B. K.; Huang, H.; Wu, F.; Chu, Y.; Zou, L.; Yang, M.; He, J.; Ye, L.; Han, M.; Zhao, T.; Zeng, L., 3D hierarchical graphene matrices enable stable Zn anodes for aqueous Zn batteries. *Nat Commun* **2023,** *14* (1), 4205.
41. Guo, W.; Cong, Z.; Guo, Z.; Chang, C.; Liang, X.; Liu, Y.; Hu, W.; Pu, X., Dendrite-free Zn anode with dual channel 3D porous frameworks for rechargeable Zn batteries. *Energy Storage Mater.* **2020,** *30*, 104-112.
42. Zhao, Z.; Wang, R.; Peng, C.; Chen, W.; Wu, T.; Hu, B.; Weng, W.; Yao, Y.; Zeng, J.; Chen, Z.; Liu, P.; Liu, Y.; Li, G.; Guo, J.; Lu, H.; Guo, Z., Horizontally arranged zinc platelet electrodeposits modulated by fluorinated covalent organic framework film for high-rate and durable aqueous zinc ion batteries. *Nat Commun* **2021,** *12* (1), 6606.
43. Zhang, Y.; Bi, S.; Niu, Z.; Zhou, W.; Xie, S., Design of Zn anode protection materials for mild aqueous Zn-ion batteries. *Energy Materials* **2022,** *2* (2), 200012.
44. Du, Y.; Feng, Y.; Li, R.; Peng, Z.; Yao, X.; Duan, S.; Liu, S.; Jun, S. C.; Zhu, J.; Dai, L.; Yang, Q.; Wang, L.; He, Z., Zinc-Bismuth Binary Alloy Enabling High-Performance Aqueous Zinc Ion Batteries. *Small* **2023**, e2307848.
45. Wang, T.; Tang, Y.; Yu, M.; Lu, B.; Zhang, X.; Zhou, J., Spirally Grown Zinc-Cobalt Alloy Layer Enables Highly Reversible Zinc Metal Anodes. *Adv. Funct. Mater.* **2023,** *33* (51), 2306101.
46. Wang, S. B.; Ran, Q.; Yao, R. Q.; Shi, H.; Wen, Z.; Zhao, M.; Lang, X. Y.; Jiang, Q., Lamella-nanostructured eutectic zinc-aluminum alloys as reversible and dendrite-free anodes for aqueous rechargeable batteries. *Nat Commun* **2020,** *11* (1), 1634.
47. Yang, J.; Yin, B.; Sun, Y.; Pan, H.; Sun, W.; Jia, B.; Zhang, S.; Ma, T., Zinc Anode for Mild Aqueous Zinc-Ion Batteries: Challenges, Strategies, and Perspectives. *Nanomicro Lett* **2022,** *14* (1), 42.
48. Yang, Q.; Liang, G.; Guo, Y.; Liu, Z.; Yan, B.; Wang, D.; Huang, Z.; Li, X.; Fan, J.; Zhi, C., Do Zinc Dendrites Exist in Neutral Zinc Batteries: A Developed Electrohealing Strategy to In Situ Rescue In-Service Batteries. *Adv. Mater.* **2019,** *31* (43), e1903778.
49. Zhou, M.; Guo, S.; Fang, G.; Sun, H.; Cao, X.; Zhou, J.; Pan, A.; Liang, S., Suppressing by-product via stratified adsorption effect to assist highly reversible zinc anode in aqueous electrolyte. *J. Energy Chem.* **2021,** *55*,

549-556.
50. Zhao, X.; Zhang, X.; Dong, N.; Yan, M.; Zhang, F.; Mochizuki, K.; Pan, H., Advanced Buffering Acidic Aqueous Electrolytes for Ultra-Long Life Aqueous Zinc-Ion Batteries. *Small* **2022,** *18* (21), e2200742.
51. Han, D.; Sun, T.; Zhang, R.; Zhang, W.; Ma, T.; Du, H.; Wang, Q.; He, D.; Zheng, S.; Tao, Z., Eutectic Electrolytes with Doubly-Bound Water for High-Stability Zinc Anodes. *Adv. Funct. Mater.* **2022,** *32* (52), 2209065.
52. Yang, K.; Fu, H.; Duan, Y.; Ma, Z.; Wang, D.; Li, B.; Park, H. S.; Ho, D., Poloxamer Pre-solvation Sheath Ion Encapsulation Strategy for Zinc Anode–Electrolyte Interfaces. *ACS Energy Lett.* **2023,** *9* (1), 209-217.
53. Zhou, L.; Wang, F.; Yang, F.; Liu, X.; Yu, Y.; Zheng, D.; Lu, X., Unshared Pair Electrons of Zincophilic Lewis Base Enable Long-life Zn Anodes under "Three High" Conditions. *Angew. Chem. Int. Ed.* **2022,** *61* (40), e202208051.
54. Zhang, Q.; Ma, Y.; Lu, Y.; Ni, Y.; Lin, L.; Hao, Z.; Yan, Z.; Zhao, Q.; Chen, J., Halogenated Zn(2+) Solvation Structure for Reversible Zn Metal Batteries. *J. Am. Chem. Soc.* **2022,** *144* (40), 18435-18443.
55. Zhang, Q.; Ma, Y.; Lu, Y.; Zhou, X.; Lin, L.; Li, L.; Yan, Z.; Zhao, Q.; Zhang, K.; Chen, J., Designing Anion-Type Water-Free Zn(2+) Solvation Structure for Robust Zn Metal Anode. *Angew. Chem. Int. Ed.* **2021,** *60* (43), 23357-23364.
56. von Wald Cresce, A.; Borodin, O.; Xu, K., Correlating Li+ Solvation Sheath Structure with Interphasial Chemistry on Graphite. *J. Phys. Chem. C* **2012,** *116* (50), 26111-26117.
57. Hu, Y.; Yang, J.; Hu, J.; Wang, J.; Liang, S.; Hou, H.; Wu, X.; Liu, B.; Yu, W.; He, X.; Kumar, R. V., Synthesis of Nanostructured PbO@C Composite Derived from Spent Lead-Acid Battery for Next-Generation Lead-Carbon Battery. *Adv. Funct. Mater.* **2018,** *28* (9), 1705294.
58. Khor, A.; Leung, P.; Mohamed, M. R.; Flox, C.; Xu, Q.; An, L.; Wills, R. G. A.; Morante, J. R.; Shah, A. A., Review of zinc-based hybrid flow batteries: From fundamentals to applications. *Mater. Today Energy* **2018,** *8*, 80-108.
59. Wang, M.; Zheng, X.; Zhang, X.; Chao, D.; Qiao, S. Z.; Alshareef, H. N.; Cui, Y.; Chen, W., Opportunities of Aqueous Manganese-Based Batteries with Deposition and Stripping Chemistry. *Adv. Energy Mater.* **2020,** *11* (5), 2002904.
60. Pan, Y.; Liu, Z.; Liu, S.; Qin, L.; Yang, Y.; Zhou, M.; Sun, Y.; Cao, X.; Liang, S.; Fang, G., Quasi-Decoupled Solid–Liquid Hybrid Electrolyte for Highly Reversible Interfacial Reaction in Aqueous Zinc–Manganese Battery. *Advanced Energy Materials* **2023,** *13* (11), 2203766.
61. Yamamoto, T.; Shoji, T., Rechargeable Zn|ZnSO$_4$|MnO$_2$-type Cells. *Inorganica Chim. Acta* **1986,** *117*, L27-L28.
62. Xu, C.; Li, B.; Du, H.; Kang, F., Energetic zinc ion chemistry: the rechargeable zinc ion battery. *Angew. Chem. Int. Ed.* **2012,** *124* (4), 957–959.
63. Pan, H.; Shao, Y.; Yan, P.; Cheng, Y.; Han, K. S.; Nie, Z.; Wang, C.; Yang, J.; Li, X.; Bhattacharya, P.; Mueller, K. T.; Liu, J., Reversible aqueous zinc/manganese oxide energy storage from conversion reactions. *Nat. Energy* **2016,** *1* (5), 16039.
64. Zuo, Y.; Meng, T.; Tian, H.; Ling, L.; Zhang, H.; Zhang, H.; Sun, X.; Cai, S., Enhanced H(+) Storage of a MnO(2) Cathode via a MnO(2) Nanolayer Interphase Transformed from Manganese Phosphate. *ACS Nano* **2023,** *17* (6), 5600-5608.
65. Zhang, A.; Zhao, R.; Wang, Y.; Yue, J.; Yang, J.; Wang, X.; Wu, C.; Bai, Y., Hybrid Superlattice-Triggered Selective Proton Grotthuss Intercalation in delta-MnO(2) for High-Performance Zinc-Ion Battery. *Angew. Chem. Int. Ed.* **2023,** *62* (51), e202313163.
66. Wang, Y.; Zhang, Y.; Gao, G.; Fan, Y.; Wang, R.; Feng, J.; Yang, L.; Meng, A.; Zhao, J.; Li, Z., Effectively Modulating Oxygen Vacancies in Flower-Like delta-MnO(2) Nanostructures for Large Capacity and

High-Rate Zinc-Ion Storage. *Nanomicro Lett* **2023,** *15* (1), 219.
67. Yadav, G. G.; Turney, D.; Huang, J.; Wei, X.; Banerjee, S., Breaking the 2 V Barrier in Aqueous Zinc Chemistry: Creating 2.45 and 2.8 V MnO2–Zn Aqueous Batteries. *ACS Energy Lett.* **2019,** *4* (9), 2144-2146.
68. Moon, H.; Ha, K. H.; Park, Y.; Lee, J.; Kwon, M. S.; Lim, J.; Lee, M. H.; Kim, D. H.; Choi, J. H.; Choi, J. H.; Lee, K. T., Direct Proof of the Reversible Dissolution/Deposition of Mn(2+)/Mn(4+) for Mild-Acid Zn-MnO(2) Batteries with Porous Carbon Interlayers. *Adv Sci (Weinh)* **2021,** *8* (6), 2003714.
69. Xue, T.; Fan, H. J., From aqueous Zn-ion battery to Zn-MnO2 flow battery: A brief story. *J. Energy Chem.* **2021,** *54*, 194-201.
70. Wu, D.; Housel, L. M.; King, S. T.; Mansley, Z. R.; Sadique, N.; Zhu, Y.; Ma, L.; Ehrlich, S. N.; Zhong, H.; Takeuchi, E. S.; Marschilok, A. C.; Bock, D. C.; Wang, L.; Takeuchi, K. J., Simultaneous Elucidation of Solid and Solution Manganese Environments via Multiphase Operando Extended X-ray Absorption Fine Structure Spectroscopy in Aqueous Zn/MnO(2) Batteries. *J. Am. Chem. Soc.* **2022,** *144* (51), 23405-23420.
71. Li, X.; Xu, Z.; Qian, Y.; Hou, Z., In-situ regulated competitive proton intercalation and deposition/dissolution reaction of MnO2 for high-performance flexible zinc-manganese batteries. *Energy Storage Mater.* **2022,** *53*, 72-78.
72. Yuan, Y.; Sharpe, R.; He, K.; Li, C.; Saray, M. T.; Liu, T.; Yao, W.; Cheng, M.; Jin, H.; Wang, S.; Amine, K.; Shahbazian-Yassar, R.; Islam, M. S.; Lu, J., Understanding intercalation chemistry for sustainable aqueous zinc–manganese dioxide batteries. *Nat. Sustain.* **2022,** *5* (10), 890-898.
73. Chen, H.; Dai, C.; Xiao, F.; Yang, Q.; Cai, S.; Xu, M.; Fan, H. J.; Bao, S. J., Reunderstanding the Reaction Mechanism of Aqueous Zn-Mn Batteries with Sulfate Electrolytes: Role of the Zinc Sulfate Hydroxide. *Adv. Mater.* **2022,** *34* (15), e2109092.
74. Yang, H.; Zhou, W.; Chen, D.; Liu, J.; Yuan, Z.; Lu, M.; Shen, L.; Shulga, V.; Han, W.; Chao, D., The origin of capacity fluctuation and rescue of dead Mn-based Zn–ion batteries: a Mn-based competitive capacity evolution protocol. *Energy Environ. Sci.* **2022,** *15* (3), 1106-1118.
75. Lei, J.; Yao, Y.; Wang, Z.; Lu, Y.-C., Towards high-areal-capacity aqueous zinc–manganese batteries: promoting MnO2 dissolution by redox mediators. *Energy Environ. Sci.* **2021,** *14* (8), 4418-4426.
76. Zhong, Z.; Li, J.; Li, L.; Xi, X.; Luo, Z.; Fang, G.; Liang, S.; Wang, X., Improving performance of zinc-manganese battery via efficient deposition/dissolution chemistry. *Energy Storage Mater.* **2022,** *46*, 165-174.
77. Zheng, X.; Wang, Y.; Xu, Y.; Ahmad, T.; Yuan, Y.; Sun, J.; Luo, R.; Wang, M.; Chuai, M.; Chen, N.; Jiang, T.; Liu, S.; Chen, W., Boosting Electrolytic MnO(2)-Zn Batteries by a Bromine Mediator. *Nano Lett.* **2021,** *21* (20), 8863-8871.
78. Shen, X.; Wang, X.; Zhou, Y.; Shi, Y.; Zhao, L.; Jin, H.; Di, J.; Li, Q., Highly Reversible Aqueous Zn-MnO2 Battery by Supplementing Mn2+-Mediated MnO2 Deposition and Dissolution. *Adv. Funct. Mater.* **2021,** *31* (27), 2101579.
79. Hu, Y.; Liu, Z.; Li, L.; Guo, S.; Xie, X.; Luo, Z.; Fang, G.; Liang, S., Reconstructing interfacial manganese deposition for durable aqueous zinc–manganese batteries. *Natl. Sci. Rev.* **2023,** *10* (10), nwad220.
80. Yang, H.; Zhang, T.; Chen, D.; Tan, Y.; Zhou, W.; Li, L.; Li, W.; Li, G.; Han, W.; Fan, H. J.; Chao, D., Protocol in Evaluating Capacity of Zn-Mn Aqueous Batteries: A Clue of pH. *Adv. Mater.* **2023,** *35* (24), e2300053.
81. Zeng, X.; Liu, J.; Mao, J.; Hao, J.; Wang, Z.; Zhou, S.; Ling, C. D.; Guo, Z., Toward a Reversible Mn4+/Mn2+ Redox Reaction and Dendrite-Free Zn Anode in Near-Neutral Aqueous Zn/MnO2 Batteries via Salt Anion Chemistry. *Adv. Energy Mater.* **2020,** *10* (32), 1904163.
82. Liu, Y.; Qin, Z.; Yang, X.; Liu, J.; Liu, X.-X.; Sun, X., High-Voltage Manganese Oxide Cathode with Two-Electron Transfer Enabled by a Phosphate Proton Reservoir for Aqueous Zinc Batteries. *ACS Energy Lett.* **2022,** *7* (5), 1814-1819.

83. Xue, X.; Liu, Z.; Eisenberg, S.; Ren, Q.; Lin, D.; Coester, E.; Zhang, H.; Zhang, J. Z.; Wang, X.; Li, Y., Regulated Interfacial Proton and Water Activity Enhances Mn2+/MnO2 Platform Voltage and Energy Efficiency. *ACS Energy Lett.* **2023,** *8* (11), 4658-4665.
84. Liu, C.; Chi, X.; Han, Q.; Liu, Y., A High Energy Density Aqueous Battery Achieved by Dual Dissolution/Deposition Reactions Separated in Acid-Alkaline Electrolyte. *Adv. Energy Mater.* **2020,** *10* (12), 1903589.
85. Zhong, C.; Liu, B.; Ding, J.; Liu, X.; Zhong, Y.; Li, Y.; Sun, C.; Han, X.; Deng, Y.; Zhao, N.; Hu, W., Decoupling electrolytes towards stable and high-energy rechargeable aqueous zinc–manganese dioxide batteries. *Nat. Energy* **2020,** *5* (6), 440-449.
86. Xie, C.; Li, T.; Deng, C.; Song, Y.; Zhang, H.; Li, X., A highly reversible neutral zinc/manganese battery for stationary energy storage. *Energy Environ. Sci.* **2020,** *13* (1), 135-143.
87. Liu, J.; Ye, C.; Wu, H.; Jaroniec, M.; Qiao, S. Z., 2D Mesoporous Zincophilic Sieve for High-Rate Sulfur-Based Aqueous Zinc Batteries. *J. Am. Chem. Soc.* **2023,** *145* (9), 5384-5392.
88. Zhang, H.; Shang, Z.; Luo, G.; Jiao, S.; Cao, R.; Chen, Q.; Lu, K., Redox Catalysis Promoted Activation of Sulfur Redox Chemistry for Energy-Dense Flexible Solid-State Zn-S Battery. *ACS Nano* **2022,** *16* (5), 7344-7351.
89. Wu, W.; Wang, S.; Lin, L.; Shi, H.-Y.; Sun, X., A dual-mediator for a sulfur cathode approaching theoretical capacity with low overpotential in aqueous Zn–S batteries. *Energy Environ. Sci.* **2023,** *16* (10), 4326-4333.
90. Li, S.; Wei, Z.; Yang, J.; Chen, G.; Zhi, C.; Li, H.; Liu, Z., A High-Energy Four-Electron Zinc Battery Enabled by Evoking Full Electrochemical Activity in Copper Sulfide Electrode. *ACS Nano* **2023,** *17* (22), 22478-22487.
91. Wu, X.; Markir, A.; Ma, L.; Xu, Y.; Jiang, H.; Leonard, D. P.; Shin, W.; Wu, T.; Lu, J.; Ji, X., A Four-Electron Sulfur Electrode Hosting a Cu(2+) /Cu(+) Redox Charge Carrier. *Angew. Chem. Int. Ed.* **2019,** *58* (36), 12640-12645.
92. Dai, C.; Hu, L.; Jin, X.; Chen, H.; Zhang, X.; Zhang, S.; Song, L.; Ma, H.; Xu, M.; Zhao, Y.; Zhang, Z.; Cheng, H.; Qu, L., A Cascade Battery: Coupling Two Sequential Electrochemical Reactions in a Single Battery. *Adv. Mater.* **2021,** *33* (44), e2105480.
93. Cai, P.; Sun, W.; Chen, J.; Chen, K.; Lu, Z.; Wen, Z., High-Energy Density Aqueous Alkali/Acid Hybrid Zn–S Battery. *Adv. Energy Mater.* **2023,** *13* (28), 2301279.
94. Zhang, W.; Wang, M.; Ma, J.; Zhang, H.; Fu, L.; Song, B.; Lu, S.; Lu, K., Bidirectional Atomic Iron Catalysis of Sulfur Redox Conversion in High-Energy Flexible Zn S Battery. *Adv. Funct. Mater.* **2023,** *33* (11), 2210899.
95. Li, W.; Ma, Y.; Li, P.; Jing, X.; Jiang, K.; Wang, D., Synergistic Effect between S and Se Enhancing the Electrochemical Behavior of Se_xS_y in Aqueous Zn Metal Batteries. *Adv. Funct. Mater.* **2021,** *31* (20), 2101237.
96. Hu, Z.; Liu, Q.; Chou, S. L.; Dou, S. X., Advances and Challenges in Metal Sulfides/Selenides for Next-Generation Rechargeable Sodium-Ion Batteries. *Adv. Mater.* **2017,** *29* (48), 1700606.
97. Huang, X.; Sun, J.; Wang, L.; Tong, X.; Dou, S. X.; Wang, Z. M., Advanced High-Performance Potassium-Chalcogen (S, Se, Te) Batteries. *Small* **2021,** *17* (6), e2004369.
98. Mei, H.; Zhang, H.; Li, Z.; Zhang, L.; Lu, X.; Xu, B.; Sun, D., Enabling kinetically fast activation of carbon nanotube@nickel selenide through pore-phase dual regulation in aqueous zinc battery. *Sci. China Mater.* **2021,** *65* (4), 929-938.
99. Cui, F.; Pan, R.; Su, L.; Zhu, C.; Lin, H.; Lian, R.; Fu, R.; Zhang, G.; Jiang, Z.; Hu, X.; Pan, Y.; Hou, S.; Zhang, F.; Zhu, K.; Dong, Y.; Xu, F., Activating Selenium Cathode Chemistry for Aqueous Zinc-Ion Batteries. *Adv. Mater.* **2023,** *35* (44), e2306580.

100. Yang, Y.; Liang, S.; Zhou, J., Progress and prospect of the zinc–iodine battery. *Curr. Opin. Electrochem.* **2021,** *30*, 100761.
101. Han, L.; Huang, H.; Li, J.; Yang, Z.; Zhang, X.; Zhang, D.; Liu, X.; Xu, M.; Pan, L., Novel zinc–iodine hybrid supercapacitors with a redox iodide ion electrolyte and B, N dual-doped carbon electrode exhibit boosted energy density. *J. Mater. Chem. A* **2019,** *7* (42), 24400-24407.
102. Ma, L.; Ying, Y.; Chen, S.; Huang, Z.; Li, X.; Huang, H.; Zhi, C., Electrocatalytic Iodine Reduction Reaction Enabled by Aqueous Zinc-Iodine Battery with Improved Power and Energy Densities. *Angew. Chem. Int. Ed.* **2021,** *60* (7), 3791-3798.
103. He, Y.; Liu, M.; Chen, S.; Zhang, J., Shapeable carbon fiber networks with hierarchical porous structure for high-performance Zn-I2 batteries. *Sci. China Chem.* **2021,** *65* (2), 391-398.
104. He, J.; Hong, H.; Hu, S.; Zhao, X.; Qu, G.; Zeng, L.; Li, H., Chemisorption effect enables high-loading zinc-iodine batteries. *Nano Energy* **2024,** *119*, 109096.
105. Liu, M.; Chen, Q.; Cao, X.; Tan, D.; Ma, J.; Zhang, J., Physicochemical Confinement Effect Enables High-Performing Zinc-Iodine Batteries. *J. Am. Chem. Soc.* **2022,** *144* (47), 21683-21691.
106. Pan, H.; Li, B.; Mei, D.; Nie, Z.; Shao, Y.; Li, G.; Li, X. S.; Han, K. S.; Mueller, K. T.; Sprenkle, V.; Liu, J., Controlling Solid–Liquid Conversion Reactions for a Highly Reversible Aqueous Zinc–Iodine Battery. *ACS Energy Lett.* **2017,** *2* (12), 2674-2680.
107. Weng, G.-M.; Li, Z.; Cong, G.; Zhou, Y.; Lu, Y.-C., Unlocking the capacity of iodide for high-energy-density zinc/polyiodide and lithium/polyiodide redox flow batteries. *Energy Environ. Sci.* **2017,** *10* (3), 735-741.
108. Xie, C.; Liu, Y.; Lu, W.; Zhang, H.; Li, X., Highly stable zinc–iodine single flow batteries with super high energy density for stationary energy storage. *Energy Environ. Sci.* **2019,** *12* (6), 1834-1839.
109. Li, X.; Li, M.; Huang, Z.; Liang, G.; Chen, Z.; Yang, Q.; Huang, Q.; Zhi, C., Activating the I0/I+ redox couple in an aqueous I2–Zn battery to achieve a high voltage plateau. *Energy Environ. Sci.* **2021,** *14* (1), 407-413.
110. Zhang, K.; Yu, Q.; Sun, J.; Tie, Z.; Jin, Z., Precipitated Iodine Cathode Enabled by Trifluoromethanesulfonate Oxidation for Cathode/Electrolyte Mutualistic Aqueous Zn-I Batteries. *Adv. Mater.* **2023**, 36(6), e2309838.
111. Han, M.; Chen, D.; Lu, Q.; Fang, G., Aqueous Rechargeable Zn-Iodine Batteries: Issues, Strategies and Perspectives. *Small* **2023**, DOI: 10.1002/smll.202310293.
112. Xie, C.; Zhang, H.; Xu, W.; Wang, W.; Li, X., A Long Cycle Life, Self-Healing Zinc-Iodine Flow Battery with High Power Density. *Angew. Chem. Int. Ed.* **2018,** *57* (35), 11171-11176.
113. Mousavi, M.; Jiang, G.; Zhang, J.; Kashkooli, A. G.; Dou, H.; Silva, C. J.; Cano, Z. P.; Niu, Y.; Yu, A.; Chen, Z., Decoupled low-cost ammonium-based electrolyte design for highly stable zinc–iodine redox flow batteries. *Energy Storage Mater.* **2020,** *32*, 465-476.
114. Wang, F.; Liu, Z.; Yang, C.; Zhong, H.; Nam, G.; Zhang, P.; Dong, R.; Wu, Y.; Cho, J.; Zhang, J.; Feng, X., Fully Conjugated Phthalocyanine Copper Metal-Organic Frameworks for Sodium-Iodine Batteries with Long-Time-Cycling Durability. *Adv. Mater.* **2020,** *32* (4), e1905361.
115. Zhang, B.; Wang, D.; Hou, Y.; Yang, S.; Yang, X. H.; Zhong, J. H.; Liu, J.; Wang, H. F.; Hu, P.; Zhao, H. J.; Yang, H. G., Facet-dependent catalytic activity of platinum nanocrystals for triiodide reduction in dye-sensitized solar cells. *Sci Rep* **2013,** *3*, 1836.
116. Wu, M.; Lin, X.; Hagfeldt, A.; Ma, T., Low-cost molybdenum carbide and tungsten carbide counter electrodes for dye-sensitized solar cells. *Angew. Chem. Int. Ed.* **2011,** *50* (15), 3520-3524.
117. Yue, G.; Zhang, W.; Wu, J.; Jiang, Q., Glucose aided synthesis of molybdenum sulfide/carbon nanotubes composites as counter electrode for high performance dye-sensitized solar cells. *Electrochim. Acta* **2013,** *112*, 655-662.

118. Liu, J.; Ma, T.; Zhou, M.; Liu, S.; Xiao, J.; Tao, Z.; Chen, J., MoS2-modified graphite felt as a high performance electrode material for zinc–polyiodide redox flow batteries. *Inorg. Chem. Front.* **2019,** *6* (3), 731-735.
119. Shang, W.; Zhu, J.; Liu, Y.; Kang, L.; Liu, S.; Huang, B.; Song, J.; Li, X.; Jiang, F.; Du, W.; Gao, Y.; Luo, H., Establishing High-Performance Quasi-Solid Zn/I(2) Batteries with Alginate-Based Hydrogel Electrolytes. *ACS Appl Mater Interfaces* **2021,** *13* (21), 24756-24764.
120. Machhi, H. K.; Sonigara, K. K.; Bariya, S. N.; Soni, H. P.; Soni, S. S., Hierarchically Porous Metal-Organic Gel Hosting Catholyte for Limiting Iodine Diffusion and Self-Discharge Control in Sustainable Aqueous Zinc-I(2) Batteries. *ACS Appl Mater Interfaces* **2021,** *13* (18), 21426-21435.
121. Wu, J.; Dai, Q.; Zhang, H.; Li, X., A defect-free MOF composite membrane prepared via in-situ binder-controlled restrained second-growth method for energy storage device. *Energy Storage Mater.* **2021,** *35*, 687-694.
122. Yang, H.; Qiao, Y.; Chang, Z.; Deng, H.; He, P.; Zhou, H., A Metal-Organic Framework as a Multifunctional Ionic Sieve Membrane for Long-Life Aqueous Zinc-Iodide Batteries. *Adv. Mater.* **2020,** *32* (38), e2004240.
123. Shang, W.; Li, Q.; Jiang, F.; Huang, B.; Song, J.; Yun, S.; Liu, X.; Kimura, H.; Liu, J.; Kang, L., Boosting Zn||I(2) Battery's Performance by Coating a Zeolite-Based Cation-Exchange Protecting Layer. *Nanomicro Lett* **2022,** *14* (1), 82.
124. Li, X.; Li, N.; Huang, Z.; Chen, Z.; Liang, G.; Yang, Q.; Li, M.; Zhao, Y.; Ma, L.; Dong, B.; Huang, Q.; Fan, J.; Zhi, C., Enhanced Redox Kinetics and Duration of Aqueous I(2) /I(-) Conversion Chemistry by MXene Confinement. *Adv. Mater.* **2021,** *33* (8), e2006897.
125. Wang, F.; Tseng, J.; Liu, Z.; Zhang, P.; Wang, G.; Chen, G.; Wu, W.; Yu, M.; Wu, Y.; Feng, X., A Stimulus-Responsive Zinc-Iodine Battery with Smart Overcharge Self-Protection Function. *Adv. Mater.* **2020,** *32* (16), e2000287.
126. Lin, D.; Rao, D.; Chiovoloni, S.; Wang, S.; Lu, J. Q.; Li, Y., Prototypical Study of Double-Layered Cathodes for Aqueous Rechargeable Static Zn-I(2) Batteries. *Nano Lett.* **2021,** *21* (9), 4129-4135.
127. Alghamdi, N. S.; Rana, M.; Peng, X.; Huang, Y.; Lee, J.; Hou, J.; Gentle, I. R.; Wang, L.; Luo, B., Zinc-Bromine Rechargeable Batteries: From Device Configuration, Electrochemistry, Material to Performance Evaluation. *Nanomicro Lett* **2023,** *15* (1), 209.
128. Wu, W.; Xu, S.; Lin, Z.; Lin, L.; He, R.; Sun, X., A polybromide confiner with selective bromide conduction for high performance aqueous zinc-bromine batteries. *Energy Storage Mater.* **2022,** *49*, 11-18.
129. Wei, H.; Qu, G.; Zhang, X.; Ren, B.; Li, S.; Jiang, J.; Yang, Y.; Yang, J.; Zhao, L.; Li, H.; Zhi, C.; Liu, Z., Boosting aqueous non-flow zinc–bromine batteries with a two-dimensional metal–organic framework host: an adsorption-catalysis approach. *Energy Environ. Sci.* **2023,** *16* (9), 4073-4083.
130. Zhang, Y.; Wei, C.; Wu, M.-X.; Wang, Y.; Jiang, H.; Zhou, G.; Tang, X.; Liu, X., A high-performance COF-based aqueous zinc-bromine battery. *Chem. Eng. J.* **2023,** *451*, 138915.
131. Li, X.; Li, N.; Huang, Z.; Chen, Z.; Zhao, Y.; Liang, G.; Yang, Q.; Li, M.; Huang, Q.; Dong, B.; Fan, J.; Zhi, C., Confining Aqueous Zn-Br Halide Redox Chemistry by Ti(3)C(2)T(X) MXene. *ACS Nano* **2021,** *15* (1), 1718-1726.
132. P. M. HOOBIN, K. J. C., J. O. NIERE, Stability of zinc/bromine battery electrolytes. *J. Appl. Electrochem.* **1989,** *19*, 943.
133. Jimenez-Blasco, U.; Moreno, E.; Colera, M.; Diaz-Carrasco, P.; Arrebola, J. C.; Caballero, A.; Morales, J.; Vargas, O. A., Enhanced Performance of Zn/Br Flow Battery Using N-Methyl-N-Propylmorpholinium Bromide as Complexing Agent. *Int J Mol Sci* **2021,** *22* (17), 9288.
134. Schneider, M.; Rajarathnam, G. P.; Easton, M. E.; Masters, A. F.; Maschmeyer, T.; Vassallo, Anthony M.,

The influence of novel bromine sequestration agents on zinc/bromine flow battery performance. *RSC Advances* **2016,** *6* (112), 110548-110556.
135. Kim, R.; Yuk, S.; Lee, J.-H.; Choi, C.; Kim, S.; Heo, J.; Kim, H.-T., Scaling the water cluster size of Nafion membranes for a high performance Zn/Br redox flow battery. *J. Membr. Sci.* **2018,** *564*, 852-858.
136. Zhang, L.; Zhang, H.; Lai, Q.; Li, X.; Cheng, Y., Development of carbon coated membrane for zinc/bromine flow battery with high power density. *J. Power Sources* **2013,** *227*, 41-47.
137. Wang, C.; Li, X.; Xi, X.; Xu, P.; Lai, Q.; Zhang, H., Relationship between activity and structure of carbon materials for Br2/Br− in zinc bromine flow batteries. *RSC Advances* **2016,** *6* (46), 40169-40174.
138. Suresh, S.; Ulaganathan, M.; Venkatesan, N.; Periasamy, P.; Ragupathy, P., High performance zinc-bromine redox flow batteries: Role of various carbon felts and cell configurations. *J. Energy Storage* **2018,** *20*, 134-139.
139. Xiang, H. X.; Tan, A. D.; Piao, J. H.; Fu, Z. Y.; Liang, Z. X., Efficient Nitrogen-Doped Carbon for Zinc-Bromine Flow Battery. *Small* **2019,** *15* (24), e1901848.
140. Choi, Y.; Hwang, J.; Kim, K. M.; Jana, S.; Lee, S. U.; Chae, J.; Chang, J., Time Transient Electrochemical Monitoring of Tetraalkylammonium Polybromide Solid Particle Formation: Observation of Ionic Liquid-to-Solid Transitions. *Anal. Chem.* **2019,** *91* (9), 5850-5857.
141. Jeon, J.-D.; Yang, H. S.; Shim, J.; Kim, H. S.; Yang, J. H., Dual function of quaternary ammonium in Zn/Br redox flow battery: Capturing the bromine and lowering the charge transfer resistance. *Electrochim. Acta* **2014,** *127*, 397-402.
142. Yan, Z.; Wang, E.; Jiang, L.; Sun, G., Superior cycling stability and high rate capability of three-dimensional Zn/Cu foam electrodes for zinc-based alkaline batteries. *RSC Advances* **2015,** *5* (102), 83781-83787.
143. He, Z.; Guo, J.; Xiong, F.; Tan, S.; Yang, Y.; Cao, R.; Thompson, G.; An, Q.; De Volder, M.; Mai, L., Re-imagining the daniell cell: ampere-hour-level rechargeable Zn-Cu batteries. *Energy Environ Sci* **2023,** *16* (12), 5832-5841.
144. Xu, C.; Lei, C.; Li, J.; He, X.; Jiang, P.; Wang, H.; Liu, T.; Liang, X., Unravelling rechargeable zinc-copper batteries by a chloride shuttle in a biphasic electrolyte. *Nat Commun* **2023,** *14* (1), 2349.
145. Liu, W.; Hao, J.; Xu, C.; Mou, J.; Dong, L.; Jiang, F.; Kang, Z.; Wu, J.; Jiang, B.; Kang, F., Investigation of zinc ion storage of transition metal oxides, sulfides, and borides in zinc ion battery systems. *Chem Commun (Camb)* **2017,** *53* (51), 6872-6874.
146. Yuan, Z.; Liu, X.; Xu, W.; Duan, Y.; Zhang, H.; Li, X., Negatively charged nanoporous membrane for a dendrite-free alkaline zinc-based flow battery with long cycle life. *Nat Commun* **2018,** *9* (1), 3731.
147. Gong, K.; Ma, X.; Conforti, K. M.; Kuttler, K. J.; Grunewald, J. B.; Yeager, K. L.; Bazant, M. Z.; Gu, S.; Yan, Y., A zinc–iron redox-flow battery under $100 per kW h of system capital cost. *Energy Environ. Sci.* **2015,** *8* (10), 2941-2945.
148. Chang, S.; Ye, J.; Zhou, W.; Wu, C.; Ding, M.; Long, Y.; Cheng, Y.; Jia, C., A low-cost SPEEK-K type membrane for neutral aqueous zinc-iron redox flow battery. *Surf. Coat. Technol.* **2019,** *358*, 190-194.
149. Yang, M.; Xu, Z.; Xiang, W.; Xu, H.; Ding, M.; Li, L.; Tang, A.; Gao, R.; Zhou, G.; Jia, C., High performance and long cycle life neutral zinc-iron flow batteries enabled by zinc-bromide complexation. *Energy Storage Mater.* **2022,** *44*, 433-440.
150. Teng, C.; Zhang, C.; Yin, K.; Zhao, M.; Du, Y.; Wu, Q.; Lu, X., A new high-performance rechargeable alkaline Zn battery based on mesoporous nitrogen-doped oxygen-deficient hematite. *Sci. China Mater.* **2021,** *65* (4), 920-928.
151. Chen, Z.; Yang, Q.; Mo, F.; Li, N.; Liang, G.; Li, X.; Huang, Z.; Wang, D.; Huang, W.; Fan, J.; Zhi,

C., Aqueous Zinc-Tellurium Batteries with Ultraflat Discharge Plateau and High Volumetric Capacity. *Adv Mater* **2020,** *32* (42), e2001469.
152. Yang, G.; Liu, Z.; Weng, S.; Zhang, Q.; Wang, X.; Wang, Z.; Gu, L.; Chen, L., Iron carbide allured lithium metal storage in carbon nanotube cavities. *Energy Storage Mater.* **2021,** *36*, 459-465.
153. Zhu, M.; Hu, J.; Lu, Q.; Dong, H.; Karnaushenko, D. D.; Becker, C.; Karnaushenko, D.; Li, Y.; Tang, H.; Qu, Z.; Ge, J.; Schmidt, O. G., A Patternable and In Situ Formed Polymeric Zinc Blanket for a Reversible Zinc Anode in a Skin-Mountable Microbattery. *Adv. Mater.* **2021,** *33* (8), e2007497.
154. Yuan, X.; Mo, J.; Huang, J.; Liu, J.; Liu, C.; Zeng, X.; Zhou, W.; Yue, J.; Wu, X.; Wu, Y., An Aqueous Hybrid Zinc-Bromine Battery with High Voltage and Energy Density. *ChemElectroChem* **2020,** *7* (7), 1531-1536.
155. Chen, H.; Wang, C.; Dai, Y.; Qiu, S.; Yang, J.; Lu, W.; Chen, L., Rational Design of Cathode Structure for High Rate Performance Lithium-Sulfur Batteries. *Nano Lett.* **2015,** *15* (8), 5443-5448.
156. Beladi-Mousavi, S. M.; Pumera, M., 2D-Pnictogens: alloy-based anode battery materials with ultrahigh cycling stability. *Chem. Soc. Rev.* **2018,** *47* (18), 6964-6989.